# Fuel utilization and its effect on solid oxide fuel cell performance

Rustam Singh Shekhar

A Thesis Submitted to

Indian Institute of Technology Hyderabad

In partial Fulfilment of the Requirement for

The Degree of Master of Technology



भारतीय प्रौद्योगिकी संस्थान हैदराबाद
**Indian Institute of Technology**
Hyderabad

Department of Chemical Engineering

June 2014

## Declaration

I declare that this written submission represents my ideas in my own words, and where ideas or words of others have been included, I have adequately cited and referenced the original sources. I also declare that I have adhered to all principal of academic honesty and integrity and have not misrepresent or fabricated or falsified any idea/data/fact/source in my submission. I understand that my violation of above will be will be cause of disciplinary action by the Institute and can also evoke penal action from the source that have thus not been properly cited or from whom proper permission has not been taken when needed.

Signature

(Rustam Singh Shekhar)
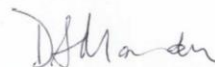
Roll no.

(CH12M1014)

## Approval sheet

This Thesis entitled **Fuel utilization and its effect on solid oxide fuel cell performance** by Rustam Singh Shekhar is approved for the degree of Master of Technology from Indian Institute of Technology Hyderabad.
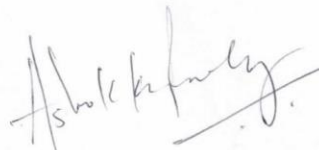

(Dr. Parag D. Pawar) Examiner

Department of Chemical Engineering

IITH


(Dr. Vinod Janardhanan) Examiner

Department of Chemical Engineering

IITH


(Dr. Dayadeep Monder) Adviser

Department of Chemical Engineering

IITH


(Dr. Ashok Kumar Pandey) External Examiner

Department of Mechanical Engineering

IITH

# Acknowledgement

# Abstract

Solid oxide fuel cells (SOFC) are energy conversion devices which have better efficiency and performance than other devices. A SOFC can operate with low noise, less harmful emissions and with higher output energy for a given amount of fuel. Fuel cells are devices which converts chemical energy directly into electrical energy. A detailed model is presented which involves all physics and examines the fuel utilization during cell operation. During operation we introduce the fuel into the cell side and unreacted fuel comes out with exhaust gases thus going waste. The fraction of fuel that is used is called fuel utilization ($U_f$) and higher $U_f$ is desirable. To increase fuel utilization we can vary the inlet fuel velocity, temperature, and other operating parameters. Microstructural properties such as electronic conductivity, ionic conductivity, triple phase boundary (TPB) length, porosity affect the cell performance directly and are themselves dependent upon the manufacturing process. We need to optimise among the properties to get desirable behaviour during cell operation since changing one parameter effects the effective electrode properties differently. Cell geometry and dimensions are also important factors in deciding performance including fuel utilization. The effect of varying various parameters for the electrodes, specifically in the anode, was investigated to suggest improved performance of the overall cell. Thickness of the anode and cathode do not affect the cell performance. The ratio of the partial pressure of water vapour to hydrogen increases with increasing utilization. This can lead to the oxidation of the nickel in the anode which is detrimental to the durability of the cell. This work shows that at 800ºC, for a fuel velocity that gives $U_f$=80% at 0.8 V, lowering the cell voltage below 0.7 V drives $U_f$ above 99%. It is only at these very severe conditions that Ni oxidation becomes favourable towards the fuel exit.

# Contents

# List of figures

# List of table

# Nomenclature

$A_{dl}$ — Contact area per unit volume of ionic and electronic conductor

$D_{ki}$ — binary diffusion coefficient ($cm^2/s$)

$d_p$ — Average particle diameter(cm)

$E_{a,H_2}$ — activation energy for $H_2$ oxidation,(J/mol)

$E_{a,O_2}$ — activation energy for $O_2$ reduction,(J/mol)

$E_{aeq}$ — equilibrium electric-potential difference in the anode,($V$)

$E_{ceq}$ — equilibrium electric-potential difference in the cathode,($V$)

$F$ — Faraday constant,($C/mol$)

$g_i$ — Gibbs free energy of components (J)

$I$ — identity matrix

$i$ — current density vector($A/cm^2$)

$i_o$ — exchange current density ($A/cm^2$)

$i_{o,a}$ — exchange current density for $H_2$ oxidation ($A/cm^2$)

$i_{o,c}$ — exchange current density for $O_2$ reduction ($A/cm^2$)

$i_{*H_2}$ — parameter in the expression of $i_{o,a}$ ($A/cm^2$)

$i_{*O_2}$ — parameter in the expression of $i_{o,c}$ ($A/cm^2$)

$i^*_{ref,H_2}$ — parameter $i^*_{H_2}$ at the reference temperature $T_{ref}$($A/cm^2$)

$i_{*ref,O_2}$ — parameter $i_{*O_2}$ at the reference temperature $T_{ref}$ ($A/cm^2$)

$j_i$ — diffusive flux $mol/cm^2s$

$M_i$ — molar mass of given species ($g/mol$)

Prat — Ration of partial pressure of hydrogen and water vapor

$P$ — pressure ($atm$)

$p$ — percentage diffusive transport in porous structure

$p_{H_2}$ — partial pressure of $H_2$ ($atm$)

$p_{O_2}$ — partial pressure of $O_2$ ($atm$)

$p_{H_2O}$ — partial pressure of $H_2O$ ($atm$)

$p_{*H_2}$ — parameter in the expression of $i_{o,a}$ ($atm$)

$p_{*O_2}$ — parameter in the expression of $i_{o,c}$ ($atm$)

$\acute{Q}_{CV}$ — Heat of control volume (J)

$R$ — universal gas constant ($J/molK$)

$d_a$ — daimeter of electrode particle ($m$)

$R_{el}$ — radius of electrolyte particle ($m$)

$\acute{S}_i$ — Entropy of componats

$T$ — Temperature ($K$)

$V_{fuel}$     average velocity  (m/s)

$w_k$     species molecular weight ($g/mol$)

$w_{CV}$     work done in control volume

$Z_{io}$     coordination number of the electrode particles

$Z_{el}$     coordination number of the electrolyte particles

$Z_\alpha$     coordination number of $\alpha$ particles

$Z_\beta$     coordination number of $\beta$ particles

$Z_{\alpha,\beta}$     coordination number of $\alpha,\beta$ particles


$\mu$     Viscosity (Kg m$^{-1}$ s$^{-1}$)

$\rho$     Density (kg m$^{-3}$ )

$\tau$     Tortuosity

$\eta_{act}$     activation losses

$\eta_{con}$     concentration losses

$\eta_{ohmic}$     ohmic losses

$\Phi$     Porosity

$\phi^{bs}$     Porosity before sintering

$\psi_{pf}^{bs}$     Pore former volume fraction before sintering

$\lambda_{TPB}$     Length of triple phase boubdary

$\alpha$     charge transfer coefficient


$\sigma_{LSM^\circ}$     electric conductivity of pure LSM, ($S/cm$)

$\sigma_{Ni^\circ}$     electric conductivity of pure Ni, ($S/cm$)

$\sigma_{YSZ^\circ}$     electric conductivity of pure YSZ, ($S/cm$)

# 1. Introduction

## 1.1 Fuel cells

Energy is present in our environment in various forms but it is very limited in amount. We need to use it very efficiently without any wastage. To use the chemical energy in readily available fuels we require conversion devices. For getting electrical energy from chemical energy we use thermal power plat, internal combustion engines. But they have low efficiency and they cause several unwanted environmental impact. Fuel cells are the devices which convert the chemical energy of the fuel directly into electrical energy without any moving parts and are eco-friendly and high efficiency devices. In fuel cells as long as we will supply fuel they can give electrical energy. Basically a fuel cell consist of three thin layers anode, cathode and electrolyte. Fuel is fed to the anode side and air to the cathode side oxidation of fuel on anode side, reduction of air in cathode side are the two reactions in a fuel cell and the ions conducted through the electrolyte layer to link these chemical reactions. Electrons conduct through the external circuit to provide desired power. We can get any amount of power from the fuel cells by assemble unit cells in a stack. The reactions below are for a solid oxide fuel cell.

Anode side (fuel oxidation reaction)

$$H_2 + O^{2-} \longrightarrow H_2O + 2e^-$$

Cathode side (oxygen reduction reaction)

$$0.5 \, O_2 + 2e^- \longrightarrow O^{2-}$$

Overall reaction

$$H_2 + 0.5 \, O_2 \longrightarrow H_2O + Energy$$
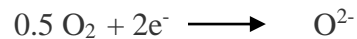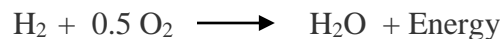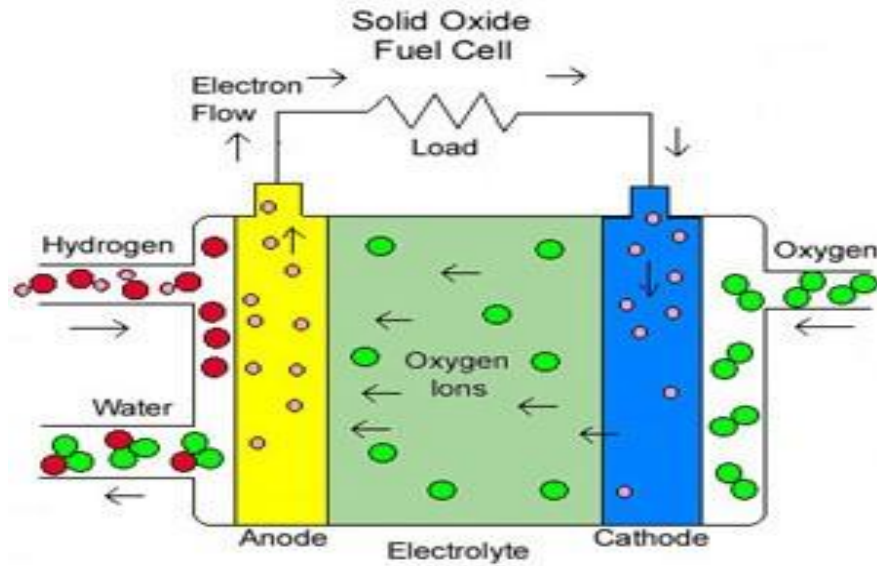
Fig. 1    Schematic of basic solid oxide fuel cell

(http://www.terienvis.nic.in/WriteReadData/links/pa-801623402)
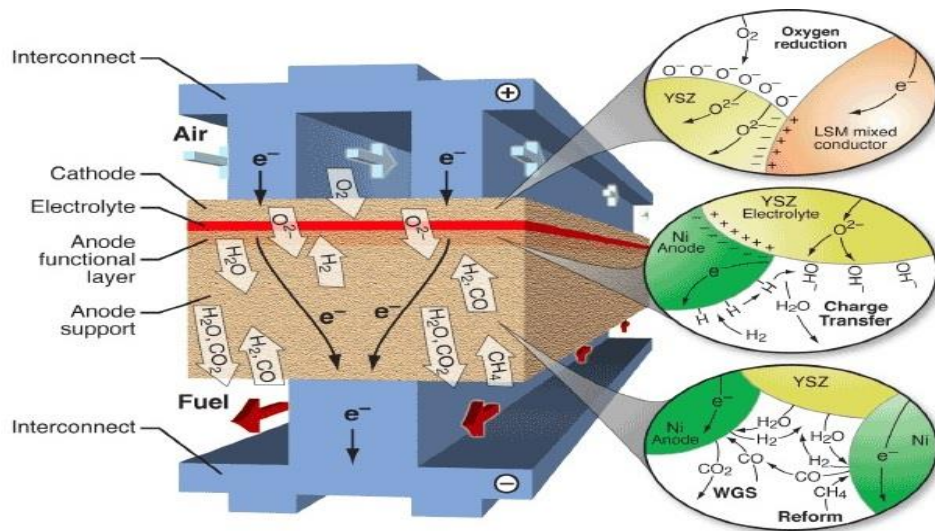


Fig. 2 Different type of conducting ions and functional layer of fuel cell.

(http://www.coloradofuelcellcenter.org/pictures/fuel_cell_modeling)

Fuel cells involves following steps for functioning:-

1. Mass transport of the fuel and air to the reaction site (anode and cathode).

2. Half reactions takes place on both electrodes.

3. Transport of the charged ions from one side to other through electrolyte.

4. Conduction of the electrons through the external circuit.

5. Removal of product to vacate the reaction sites.

Above processes are take place simultaneously when fuel cell produce current. Fuel cell uses hydrogen, methanol, hydrocarbons and syngas as fuel cell according to their operating condition and the material used for these layer in fuel cell.

## 1.2 Types of fuel cell

There are essentially 5 types of fuel cells. They are as follows:-

1. Alkaline fuel cell (AFC)

2. Phosphoric acid fuel cell (PAFC)

3. Polymer electrolyte membrane fuel cell (PEMFC)

4. Solid oxide fuel cell (SOFC)

5. Molten carbonate fuel cell (MCFC)

Some characteristics of different types of fuel cells are

| Fuel cell type | Cell component | Electrolyte | Operating temperature |
|---|---|---|---|
| PEMFC | Carbon based | Polymer membrane | 50-180 °C |
| AFC | Carbon based | Aqueous solution of potassium hydroxide | 60-220 °C |
| PAFC | Carbon based | Phosphoric acid | 200 °C |
| MCFC | Stainless based | Molten carbonate | 650 °C |
| SOFC | Ceramic based | Ceramic | 600-1000 °C |

Table 1 Types of fuel cells

We are concentrating on solid oxide fuel cell because:-

1. Relative to other fuel cell, SOFCs are more fuel flexible.

2. High temperature operation produces the exhaust gases on high temperature which can help to make hybrid system by combining with gas turbine or steam turbine to recover exhaust heat.

3. It is ideal for carbon capture without substantial additional cost because the air kept separated by design from the exhaust fuel steam.

4. It offers the highest efficiency

## 1.3 Solid oxide fuel cell

Solid oxide fuel cells are high temperature fuel cells generally operated at 650- 800 °C. This fuel cell mainly made of ceramic. Conducting ion through electrolyte is oxide ions. This fuel cells are highly fuel flexible. We can use directly methanol, carbon monoxide, syngas and higher hydrocarbon as fuel.

SOFC consist two flow channel air and fuel flow channel with three functional layer. At anode side we are providing humidified fuel and at cathode side we are providing air from the atmosphere. While operation of the cell there we have inlet and outlet are provided according to the geometry for the fuel and air. Both gases come and passes through the channel where fuel and air need to be diffuse through the porous electrodes and reaches to the reaction site and reacts there to give energy and water product but rest of the fuel goes waste leave through the exhaust provided.

## 1.4 Motivation

In SOFC we uses humidified hydrogen, hydrocarbons as fuel. These are costly and exists in limited in nature. We need to use these fuel efficiently and precisely. During the operation of SOFC we provides the fuel at high flow rate to get more current density. In this process we can see that fuel goes waste from exhaust because of many reasons. Wastage of fuel is not desirable therefore we worked on an efficient model building to increase the utilization of the fuel and reduce the wastage. But because of high utilization of fuel we observed some structural and operational problem in the cell. In this thesis we tried to get the best mathematical model for the higher utilization with minimal negative effects and simulated for various working conditions and parameter to our objective.

## 1.5 Objective of thesis

In this thesis we mainly focused on the increasing the fuel utilization by changing the microstructure properties, operating conditions. And observe the negative effects on the cell structure and its performance.

# 2. System model

## 2.1 Introduction

Fuel cells are having the wide range of operating conditions, manufacturing material and output power depends upon assembly of cell. For our modelling purpose we model a simple planner cell and triple functional layer geometry as anode, cathode and electrolyte. In this thesis our work is concentrated for fuel utilization so we worked on the anode layer and we model it for the best performance. This model is anode supported type fuel cell which means we keep anode thicker than other two layers. We simulated first with thick anode 10 times thicker than the cathode and simulated it for various parameters. And find that the thicker anode cause of losses in fuel mainly transport losses. We introduced a support layer to the anode which is offering less transport losses and enhancing the performance. Support layer helps in minimize the losses because of less porosity and high permeability to the diffusing gasses. Microstructural properties of anode, cathode and electrolyte are also modelled to minimize losses. Microstructural properties as porosity, tortuosity, electrical conductivity, and ionic conductivity, contact area per unit volume of ionic and electronic conductor in anode and cathode, length of triple phase boundary (TPB), average particle diameter are calculated from the fabrication method of the electrodes. Electrode are fabricated by the sintering of the material.



Fig. 3 Layers of SOFC

Mathematical model of fuel cell can be built with various time scale and length scale. Cell can be modelled from the surface chemistry of the electrodes to system level modelling. In our model we started from the surface chemistry of the reaction sites and cover up to a unit cell model. Our

model consists surface chemistry behaviour of the molecule, microstructure of the electrodes and electrolyte, electrode modelling for the various physics which incorporate with the operation of the cell and after coupling of all physics and the model we got the entire cell behaviour with minimum assumption which makes the behaviour as the real cell. In this model we include the electrochemical reaction, transport of chemical species, charge transfer from one side to another side, current generation. Our fuel cell model is a multi-scale and multiphysics model.
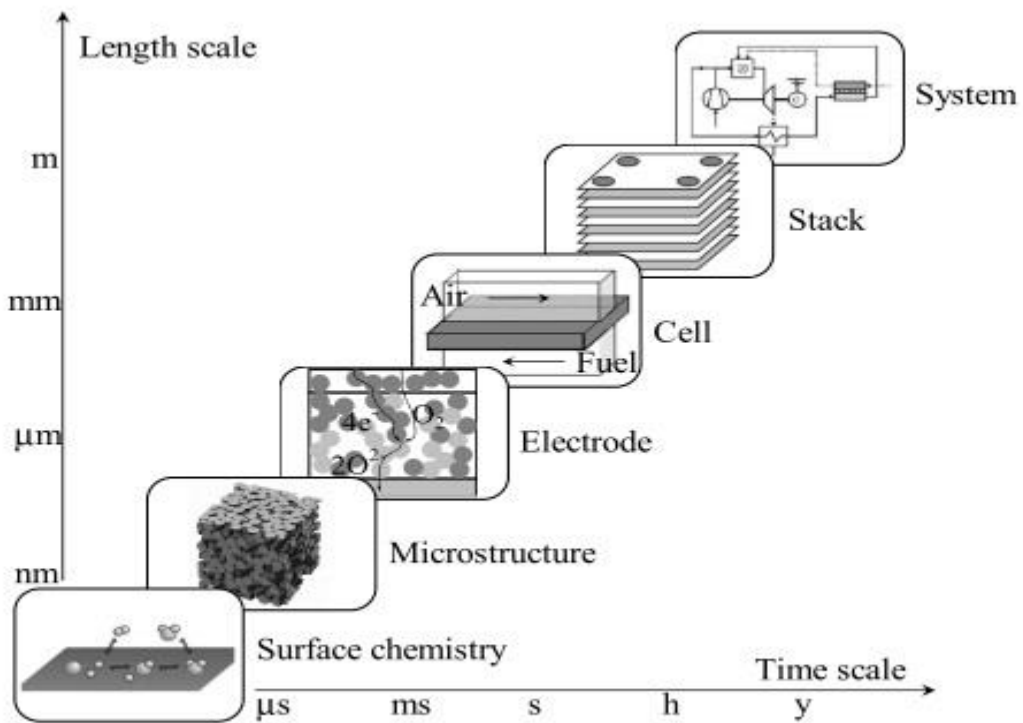


Fig .4 Scale of modelling of fuel cell with time and length (Bertie thesis [8], mathematical modelling of solid oxide fuel cell)

We can describe our model on the basis as follows:-

## 2.2 Microstructure of electrode

We used the model which described in the bertie thesis of electrode microstructure and its properties from its fabrication method. Our cell is fabricated by the high temperature sintering method. In this method we mixed pore former material (Graphite) with the ionic and electronic conductor material during the electrode fabrication. Pore former material decompose at the high temperature sintering of mixture of powder. This pore former material after decomposition leaves the extra pores on the microstructure. The volume fractions of all three material decide the properties of electrode microstructure. Estimation of the properties of the material is descried bye the extended percolation theory. By this theory we can relate the pore former volume to the final porosity and then subsequently the other microstructure properties of the electrodes. All claulation of the microstructure properties taken form the bertie thesis. Porosity can be given as below.

$$\phi = \psi_{pf}^{bs} * \left(1 - \phi^{bs}\right) + \phi^{bs} \qquad (1)$$

Where $\phi$ porosity is after sintering, $\psi_{pf}^{bs}$ pore former volume fraction before sintering and $\phi^{bs}$ is the porosity before sintering.
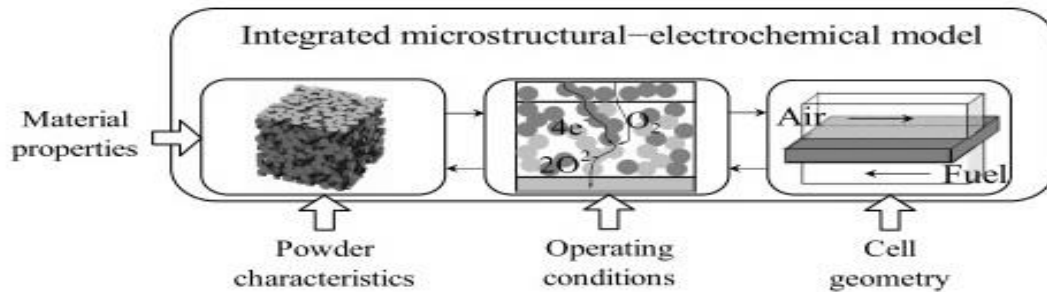


Fig. 5 Integrated microstructural model (Bertie thesis [8], mathematical modelling of solid oxide fuel cell)

On the basis of the final porosity after sintering we can calculate the volume fraction of ionic and electronic conductor volume fraction after sintering to obtain the other microstructure properties.

Tortuosity of the micro structure

$$\tau = 1 - p * log(\phi) \tag{2}$$

Where $\tau$ is tortuosity, p is percentage diffusive transport in porous structure

Length of triple phase boundary per unit volume:-

$$\lambda_{TPB} = 6(1 - \phi^{bs})\gamma_{el}^0\gamma_{io}^0 \frac{\psi_{pf}^{bs}}{d_{el}^3} Z_{el,io}d_c \tag{3}$$

Where $\lambda_{TPB}$ the length of triple phase boundary is, $d_{el}$ is the diameter of electric conductor particle diameter.

Effective electric properties of the microstructure:-

$$\sigma_{el}^{eff} = \sigma_{el}\big((1 - \phi)\psi_{el}\gamma_{el}\big)^{1.5} \tag{4.1}$$

$$\sigma_{io}^{eff} = \sigma_{io}\big((1 - \phi)\psi_{io}\gamma_{io}\big)^{1.5} \tag{4.2}$$

Where $\sigma_{el}^{eff}, \sigma_{io}^{eff}$ the effective conductivity are after sintering of electronic and ionic conductor respectively, $\psi_{io}, \psi_{el}$ are the volume fraction of ionic and electronic conductor after sintering and $\sigma_{io}, \sigma_{el}$ are the conductivity of ionic and electrical conductors in the pure form before sintering.

## 2.3 Losses in fuel cell

Entropy generation term we identified as the losses in the system during operation we have generally 3 types of losses which are:-

1. Activation losses

2. Ohmic losses

3. Concentration losses

Loses of fuel cell are describe as:-

Activation losses: - activation loss is loss which occurs because of the electrochemical reaction of the cell. In every chemical reaction we need activation energy to initiate the reaction. So we do need the same for the electrochemical reaction also.it occurs on the both side of the cell.

Ohmic losses: - Ohmic loss occurs because of resistance in flow of ions through electrolyte and electron thorough interconnect and external circuit. Because of the resistance we can see the drop in the voltage.

Concentration losses: - concentration losses occurs at high current drag when we need to supply more fuel to the ration site but because of transport limitation of species we can see the concentration losses.

## 2.4 Electrochemistry of SOFC

Fuel cell get chemical energy and convert into the electrical energy. Electrochemical reaction occurs on the surface of the electrodes. Electrochemical reaction produces the electrons which conducts through the external circuit which produces current

In SOFC current generation is directly proportional to the chemical reaction of the chemical species. Current generation in the fuel cell described by the Butler-Volmer equation

$$i = i_{o,in} \left\{ \frac{c_{H_2}}{c_{H_2,in}} e^{-\frac{\alpha F}{RT} \eta_{in}} - \frac{c_{H_2}}{c_{H_2O_{in}}} e^{\frac{(1-\alpha)F}{RT} \eta_{in}} \right\} \qquad (5)$$

Where i is the current density defined as (i =I /A where A is the apparent area of the electrode where the current is generating), $i_0$ in is called the exchange current density and is a function of T and inlet fuel composition. $C_{H2}$ is the concentration of $H_2$ and $C_{H2O}$ is the concentration of $H_2O$, α is the symmetry or charge transfer coefficient and $\eta_{in}$ = E − $E_{in}$ is the anode activation over potential. E is the operating anode potential and E in is the equilibrium anode potential at fuel inlet conditions. Rate of current generation is proportional to current generated can be given as:-

$$r_i = \frac{I}{n_i F}$$

Where r is the rate of reaction, n is the electrons participating and F is called Faraday constant.

## 2.5 Transport of chemical species

Chemical species we are feeding to the fuel cell for producing the current. We are giving fuel and air through the channels. In our model we consider humidified hydrogen as fuel (97% hydrogen and 3% water vapour) and at cathode side we have air which consist of oxygen and nitrogen so there we have binary diffusion both side. At anode hydrogen is converting into the water vapour so the composition is also changes as reaction proceeds. Frist of all at both side gases need to diffuse through free media and then it have to diffuse through porous electrode to reach reaction sits where the reaction occur. In the channels the transport of the species manly occurs by the convection of gasses with contribution of the diffusion. In porous electrodes we have transport of species mainly because of the diffusion and both side has two gasses so the diffusion of the gasses can be described by the binary Maxwell Stefan diffusion.

To make diffusion faster we need to make electrode as thin as possible so we kept our electrode thin and to give mechanical support to the cell introduced the porous support layer with higher porosity with respect to rest of the electrode. To calculate diffusion of binary components, binary diffusion constant is needed for the given operating condition as follows:-

$$D_{a-b} = \frac{K_d T^{1.75}}{P\left(v_a^{\frac{3}{2}} + v_b^{\frac{3}{2}}\right)^2 \sqrt{\frac{1}{M_a} + \frac{1}{M_b}}} \qquad (6)$$

Where a, b are the gases, T is the operating temperature, P is the total pressure, M is the molecular weight, v is the kinetic volume of gases in mixture and $K_d$ is the reference diffusivity

To calculate the effective diffusivity for the porous media and pore of electrode we can have:-

$$D_{\text{a-b,eff.}} = \frac{porosity}{tortuousity} D_{\text{a-b}}$$

## 2.6 Redox reaction in anode

We are using at anode side Ni (nickel) and YSZ (yttrium stabilised zirconia) as functional layer.

Ni is being used as the electronic conductor as well as catalyst for the anode half reaction during the reaction Ni is converting in the NiO and vise versa  reaction is as follows:-

$$NiO + H_2 \longrightarrow Ni + H_2O$$

In this reaction we need maintain forward reaction to keep converting hydrogen fuel in water vapour and Ni for catalyse the reaction. During the operation based on partial pressure oxidation and reduction of nickel occurs on the functional layer. Anode reduction increases porosity because of the NiO to Ni volume change. Reduction and oxidation of nickel will result in large bulk volume changes. In theory, the bulk volume of a fully dense NiO sample should contract by 40.9% upon reduction and should expand by 69.2% upon oxidation. It is generally believed that NiO reduction is first-order and the rate has a linear dependence with the partial pressure of hydrogen. Ni oxidation generally follows a parabolic trend at temperatures greater than 1000C with activation energies typical of the outward bulk diffusion of Ni in NiO however, at temperatures less than 1000C.

## 2.7 Triple phase boundary

In the fuel cell electrode we have pores to the flow of gases form, metal interconnect to conduction of the electron and composite material for the conduction of the oxide ions. But the reaction will occur only then when we have this three phase (gas, ionic and electrons) will be accessible to the each other if there we have triple phase boundary then only we will have a reaction and current generation. We can have reaction only on the red line which is accessible to the all three phases.
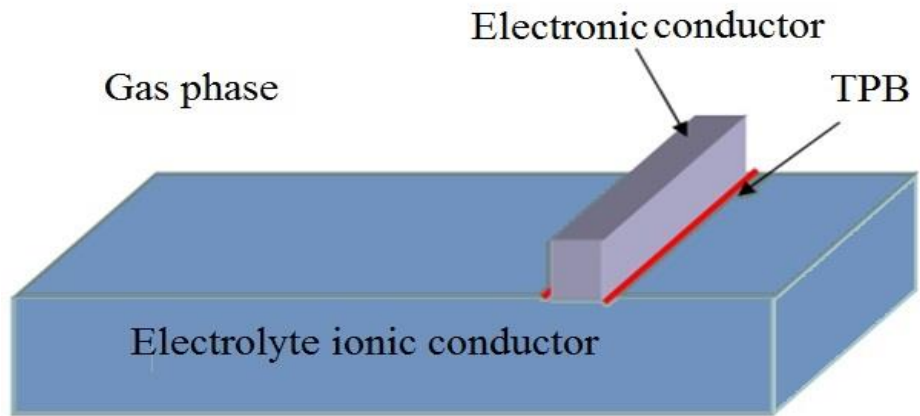
Fig.6 Triple phase boundary in the fuel cell electrodes microstructure

# 3. Multiphysics modelling of SOFC

We model the SOFC using comsol multiphysics modelling and simulation tool. We did simulation on 2D geometry of fuel cell. The thicknesses of anode electrolyte and cathode are 50, 20 and 50 micro meter respectively. We introduced a support layer with 500 micro meter

Figure 7, not drawn to scale, shows the general geometry for a planar co-flow SOFC
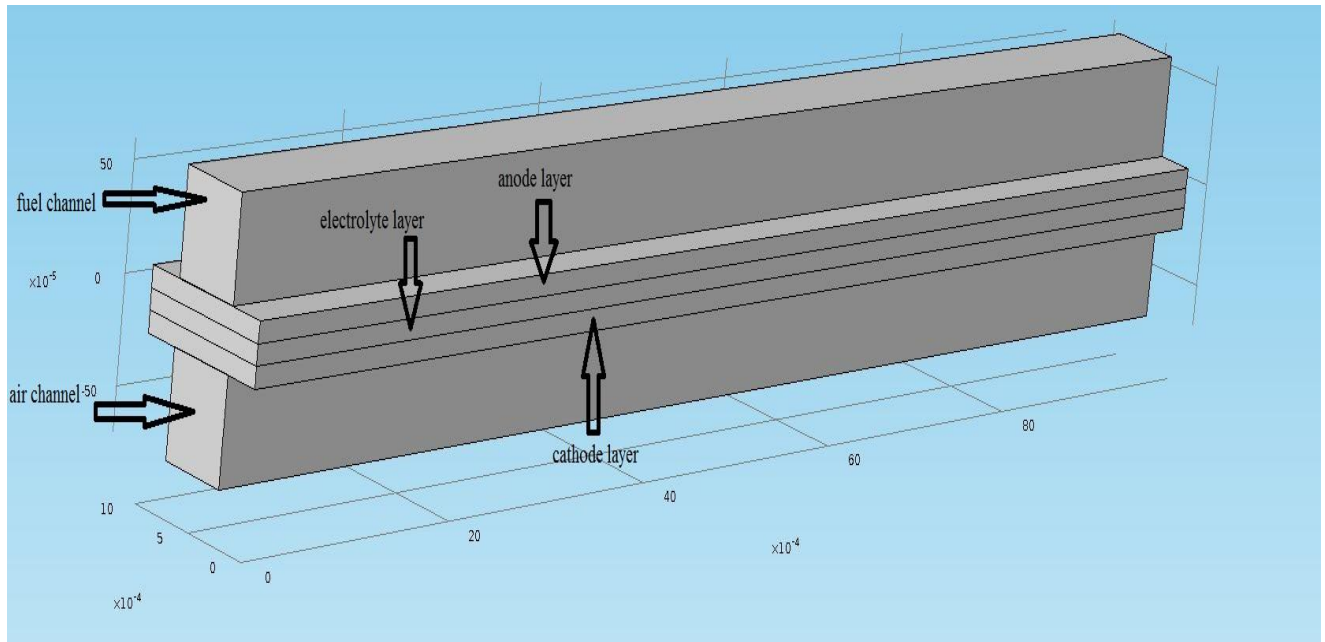


Fig.7 3-D view of cell geometry

To show the real dimensions of cell we can have the 2-D geometry of the cell. It has the extension in the flow channel to stabilize the flow and at higher current it prevents the back diffusion of the gasses in the channels which ensured the mass balance in the model.
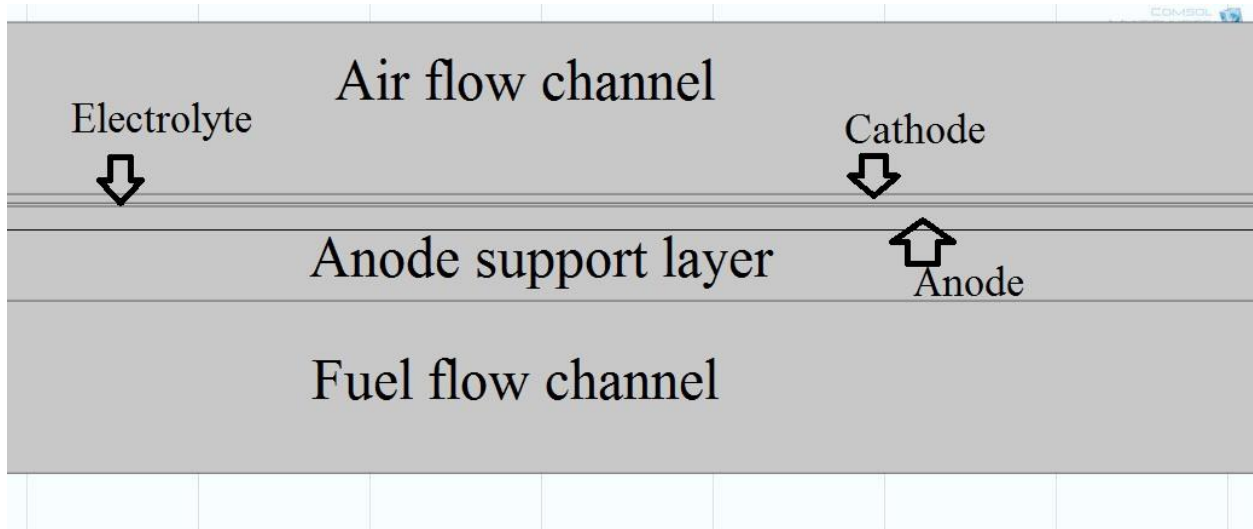
Fig. 8 Fuel cell 2-D section of actual simulated geometry

In our

modelling parts there we have main physics included in that are named as:-

1. Flow in free and porous media  (air and fuel)
2. Mass transfer in free and porous media
3. Current generation in the cell (using Poisson's equation )

## 3.1 Flow of species in free and porous media

Modelling the flow in the fuel channel and porous media we solved the Navier-Stokes equation with consideration of compressible flow.

$$\rho(v.\nabla)v = -\nabla p - \left[\mu(\nabla v + (\nabla v)^T) - \frac{2}{3}\mu(\nabla.v)I\right]$$

(7)

$$\nabla.(\rho v) = 0$$

$$\frac{\mu}{\kappa}v = -\nabla p - \frac{1}{\varepsilon}\nabla\left[\mu(\nabla v + (\nabla v)^T) - \frac{2}{3}\mu(\nabla.v)I\right]$$

$$(8)$$

$$\nabla.(\rho v) = s_m$$

Where $s_{m\ is}$ the source term when current is produced. It is equal to current generation and It will be non-zero if volumetric current generation is allowed.

K is the permeability of flow media is calculated by the Kozeny-Carman relation

$$\kappa = \frac{\phi_g d_p^2}{72T_g(1-\phi_g)^2}$$

Where $v$ is the velocity vecter, $\mu$ is the viscosity of fluid, $\rho$ is the density which is calculated by the solver by the ideal gas law, p is the pressure and I is the identity vector

Boundary condition for this will be

- Inlet velocity
- Air and fuel are exiting at atmospheric pressure
- No slip boundary condition on the walls

## 3.2 Mass transport

We solved Maxwell Stefan equation for the binary diffusion in free and porous media

$$j_i = -\sigma\omega_i \sum_{k=1}^{n} D_{ik}\left[\nabla y_k + (y_k - w_k)\frac{\nabla p}{p}\right]$$

$$(9)$$

Where $D_{ik}$ is the relative diffusivities of the components in the free media. For the free media (channels) we will use $D_{ik}$ and for porous media (cathode and anode volume) $D_{ik,eff}$ .

Boundary conditions for the mass transport are:-

- Mole fraction of hydrogen and oxygen is specified at the inlet of channels
- No flux at the walls

## 3.3 Voltage and current distribution (poission's equation)

Using Poisson equation we solved for Ohms law and that Ohms law gives the current and voltage distribution. The ionic potential can be given by the following equations

In electrolyte

$$\nabla.(-\sigma_i \nabla \emptyset_i) = 0 \qquad (10)$$

In composite electrode

$$\nabla.\left(-\sigma^{eff}{}_i \nabla \emptyset_i\right) = i_v \qquad (11) \qquad \text{For ionic conduction}$$

$$\nabla.\left(-\sigma^{eff}{}_e \nabla \emptyset_e\right) = i_v \qquad (12) \qquad \text{For electronic conduction}$$

Where $\emptyset_i$ ionic potential, $\emptyset_e$ electronic potential, $\sigma_i$ ionic conductivity in electrolyte, $\sigma_i^{eff}$ effective ionic conductivity, $\sigma_e^{eff}$ effective electronic conductivity and $i_v$ is the volumetric current generation. Conductivities are defines as follows:-

$$\text{For YSZ} \qquad \sigma_i = \frac{5.2E7}{T} e^{\frac{-84E3}{RT}} \qquad (13)$$

$$\text{For nickel} \qquad \sigma_e = 3.27E4 - 10.653T \qquad (14)$$

$$\text{For LSM} \qquad \sigma_i = \frac{8.855E5}{T} e^{\frac{-9000}{RT}} \qquad (15)$$

Boundary condition for this are

- Electric Insulation is specified at electrode and electrolyte edges
- Electric Ground is specified at current collector of anode
- Electric potential is specified at current collector of cathode

## 3.4 Current generation

Fuel cell described by the Butler- Volmer equation

For the anode side

$$ia = i_{oA,in}\left\{\frac{c_{H_2}}{c_{H_2,in}}e^{\frac{1.5F}{RT}\eta_{an}} - \frac{c_{H_2O}}{c_{H_2O_{in}}}e^{-\frac{0.5F}{RT}\eta_{an}}\right\} \qquad (16)$$

Where $c_{H_2}$ local concentration of H$_2$ is, $\eta_{an}$ is the anodic losses. This equation tells that current is the function of local concentration of species and exchange current density ($i^{oA,\in}$). Exchange current density is the function of the temperature. Exchange current density expression taken from Zhu and Kee for both anode and cathode side

$$i_{oA,in} = i_{H2}\frac{\left(\frac{p_{H_2}}{p_{H_2}^*}\right)^{\frac{\alpha_a-1}{2}}(\frac{p_{H_2O}}{p_{atm}})^{\frac{\alpha_a}{2}}}{1+(\frac{p_{H_2}}{p_{H_2}^*})^{\frac{1}{4}}} \qquad (17)$$

Where the $p_{H_2}, p_{H_2O}$ are the partial pressure of gases, α is the symmetry parameter $i_{H2}$ is the function of temperature given below

$$i_{H2} = i_{ref,H_2}^* e^{[-\frac{E_{a,H_2}}{R}(\frac{1}{T}-\frac{1}{T_{ref}})]} \qquad (18)$$

Where $i_{ref,H_2}$ is assign empirically at the $T_{ref}$ temperature, $E_{a,H_2}$ is the activation energy for the reaction


For cathode

$$ic = i_{oC,in}\left\{e^{\frac{0.75F}{RT}\eta_{ca}} - \frac{c_{O_2}}{c_{O_2\ in}}e^{-\frac{0.25F}{RT}\eta_{ca}}\right\} \qquad (19)$$

Where $c_{O_2}$ local concentration of O$_2$ is, $\eta_{ca}$ is the cathode losses. This equation tells that current is the function of local concentration of species and exchange current density ($i^{oC,\in}$). Exchange current density is the function of the temperature.

$$i_{oC,in} = i_{O2} \frac{\left(\frac{p_{O_2}}{p_{O_2}^*}\right)^{\frac{\alpha_a}{2}}}{1 + \left(\frac{p_{O_2}}{p_{O_2}^*}\right)^{\frac{1}{2}}} \tag{20}$$

Where the $p_{O_2}$ is the partial pressure of gases, α is the symmetry parameter $i_{H2}$ is the function of temperature given below

$$i_{O2} = i_{ref,O_2}^* e^{\left[-\frac{E_{a,O_2}}{R}\left(\frac{1}{T} - \frac{1}{T_{ref}}\right)\right]} \tag{21}$$

Where $i_{ref,O_2}$ is assign empirically at the $T_{ref}$ temperature, $E_{a,O_2}$ is the activation energy for the reaction.

## 3.5 Redox reaction of nickel

Fuel cell produces water as product by consuming the hydrogen. Because of this water vapour production there we have reduction and oxidation of the nickel catalyst and electron conductor. Degradation of nickel is a cause of degradation in cell performance. To minimize the degradation of nickel we need to operate in favourable condition. Nickel redox reaction is depends on the partial pressure of the hydrogen and water vapour in the channel and porous electrode. To monitor the ration of partial of the in the channel we have a variable called Prat.
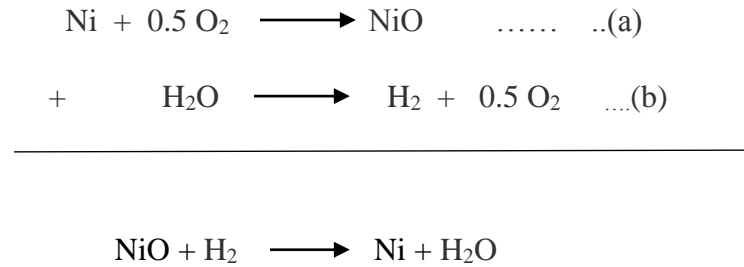
$$Prat = \frac{mole\,fraction\,of\,hydrogen}{mole\,fraction\,of\,water\,vapour}$$

For calculation of the ration of partial pressure which can prevent the nickel oxidation reaction on the anode surface can be calculated with the help of the thermodynamic feasibility of the gas. We can obtain the relationship of partial pressure and feasibility of reaction by Vant's Hoff isotherms relationship. According to this relationship for the reaction

$$NiO + H_2 \longrightarrow Ni + H_2O$$
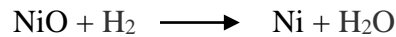
We need to calculate the ΔG of the reaction which gives the feasibility of the reaction. Where the NiO and Ni are the solids which are reacting with the gases. To calculate the ΔG of the reaction

we chosen the indirect way. We use the oxidation of the nickel with oxygen and formation of the water reaction to get the ΔG of reaction.

$$Ni + 0.5\ O_2 \longrightarrow NiO \qquad \ldots\ldots \quad ..(a)$$

$$+ \qquad H_2O \longrightarrow H_2 + 0.5\ O_2 \quad \ldots(b)$$

$$NiO + H_2 \longrightarrow Ni + H_2O$$

To calculate the ΔG of the reaction (a) we got the relation in the literature which is valid for the 911-1376 K temperature which is our operating temperature range is

$$\Delta G = \text{-55,844} + 20.290 \times T$$

And the formation of the water for our operating range we prepared a code according to NASA polynomial to calculate the thermodynamic properties and get the ΔG value of the formation of the water. The difference of both relation is the ΔG value for the nickel oxidation reaction in humid environment. According to the vant's hoff relation

$$\Delta G = \Delta G^0 + RTln(Q)$$

$$\Delta G^0 = -RTlnK \quad \text{And} \quad Q = \frac{ACTIVITY\,OF\,REACTANT}{ACTIVITY\,OF\,PRODCUT} = \frac{\partial PRESSURE\,OF\,H2O}{\partial PRESSURE\,OF\,H2}$$

 Final relation we can get as

$$\Delta G = RTln\left(\frac{Q}{K}\right)$$

Knowing the value of $\Delta G^0$ and the activities of reactants and products at any given condition, the free energy change for the equation at that condition, $\Delta G$ , can be calculated, and the thermodynamics feasibility of the reaction can be predicted.

at 1073k

H2  G = -1.5774e+05

H2O G = -4.6563e+05

O2  G = -2.3874e+05

For nickel oxydation

-55844+20.290*1073= -3.4073e+04 cal/mol

-3.4073e+04*4.183 = -1.4253e+05 j/mol

formation of water

-4.6563e+05-(-1.5774e+05+(-2.3874e+05/2)) = -188520 j/mol

for nickel oxide reduction $\Delta G^o = -1.4253e+05 + 188520 = -45990$

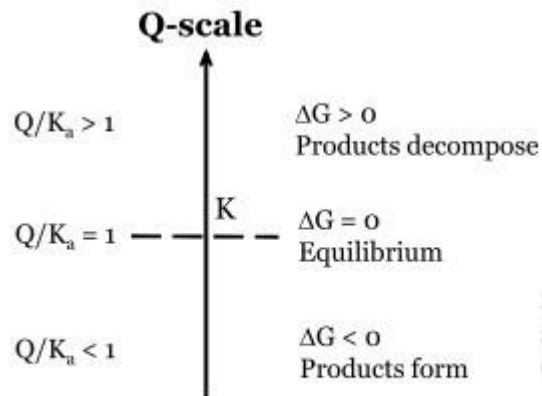Therefore K =exp ( 45990/1073/8.314) = 173.3478



Fig. 9 Sketch of the scale for the $\Delta G$ and (Q/K) showing the spontaneous change of a chemical reaction. (http://teacher.buet.ac.bd/bazlurrashid/231_nov2013/lec_24)

| Parameter | Value | Unit |
|---|---|---|
| Operating Temperature | 1073 | K |
| Operating Pressure | 1 | Atm |
| Inlet mole fraction of hydrogen | 0.97 | |
| Inlet mole fraction of water vapour | 0.03 | |
| Inlet mole fraction of oxygen | 0.21 | |
| Inlet mole fraction of nitrogen | 0.79 | |
| Inlet fuel velocity at 80% fuel utilization | 0.18162 | m/s |
| Inlet air velocity at 80% fuel utilization | 5 | m/s |
| Anode | | |
| Anode Thickness | 135 | μm |
| YSZ particle diameter | 1 | μm |
| Nickel particle diameter | 1 | μm |
| Porosity at anode | 0.52 | |
| Tortuosity at anode | 1.3270 | |
| Permeability of anode | 5.9232 e-11 | $m^2$ |
| Permeability of anode support layer | 3.9922 e-10 | $m^2$ |
| Cathode | | |
| Thickness | 50 | μm |
| LSM particle diameter | 1 | μm |
| Porosity at cathode | 0.52 | |
| Tortuosity at cathode | 1.32270 | |
| Permeability of cathode | 5.9232 e-11 | $m^2$ |
| Electrolyte | | |
| Thickness | 50 | μm |
| Electrolyte (YSZ ) conductivity | 3.9518 | s/m |

Table 2   List of operating conditions and parameter

## 3.6 Mesh and solver

After building geometry for the solving and simulating the system we do mesh for the geometry.

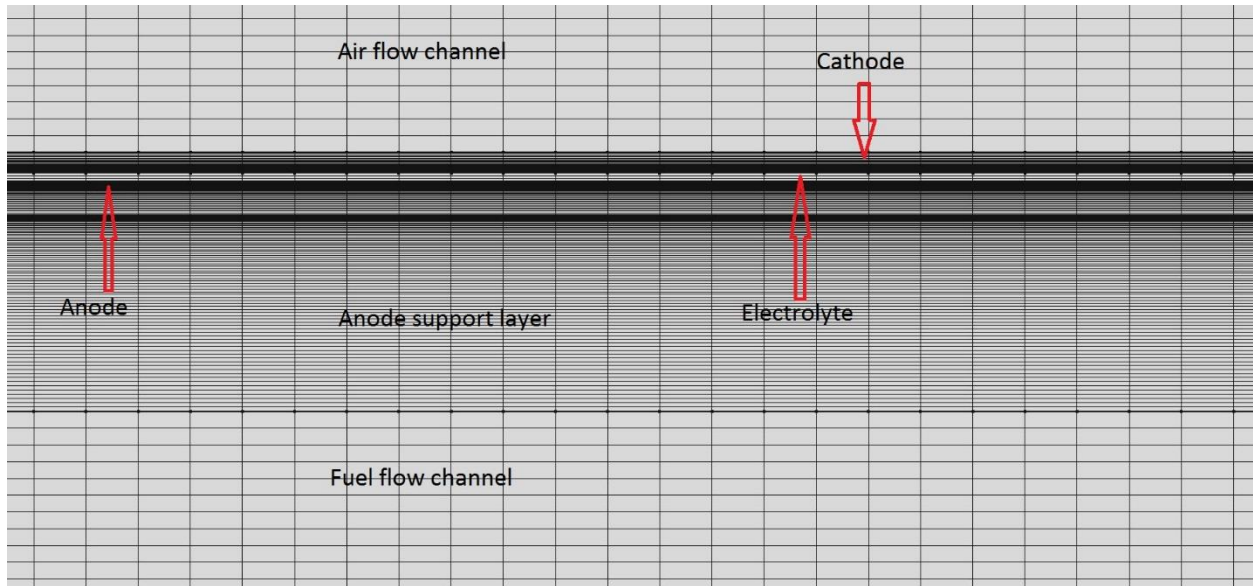We used the mapped mash method to meshing.

Fig.10 Mesh arrangement in the cell geometry

We did mesh for the fixed elements. Here we did regular mesh for the electrolyte with 3 elements. At anode and cathode side we use predefined distribution type in arithmetic sequence. We targeted denser mesh near to the electrolyte- electrode interface for better accuracy. In our mesh maximum element size is 1e-4m, minimum element size is 1.5e-5m and maximum element growth is 1.3. We solved for 80900 elements.

To solve this model we used a direct solver fully coupled for all physics together and parametric study for various parameters. We used COMSOL, MATLAB and MS excel for the post processing and interpreting the results. Tolerance for the solver is 1e-6 .it solves the all physics together until overall error comes under the tolerance.

# 4. Results and discussion

We solved for the 2-D geometry and plotted. Here we have considerable assumption is that our cell is working in isothermal condition.

Modelling of microstructure we fabricate by the high temperature sintering. We varied the pore former volume and observe the microstructure transport and electrical properties are as follows

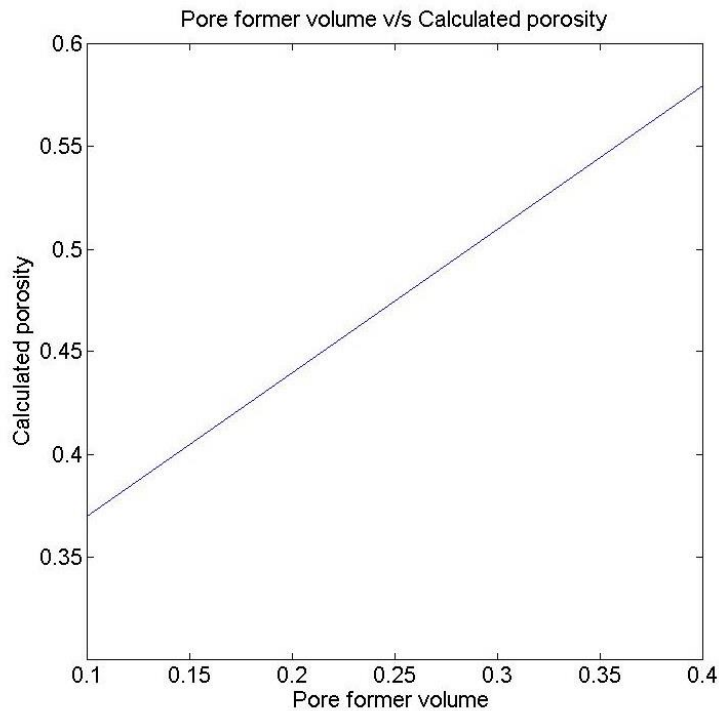By varying the pore forming volume and porosity shown in figure 11.



Fig. 11 Calculated porosity v/s pore former volume fraction with constant ratio of the ionic and electronic conductor

With increasing the pore former volume we can get the more porosity. This porosity contributes in the variation in the other cell microstructural properties.
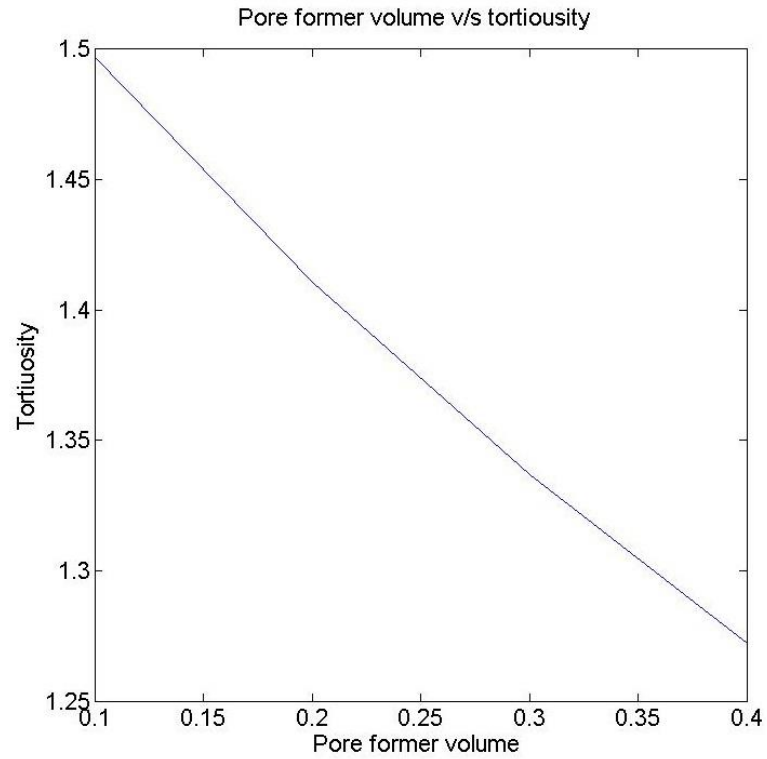
Fig. 12 Tortuosity v/s Pore former volume with constant ratio of the ionic and electronic conductor

Less tortuosity helps in the transport of species through the pore but with this desirable changes we get some undesirable property changes also.
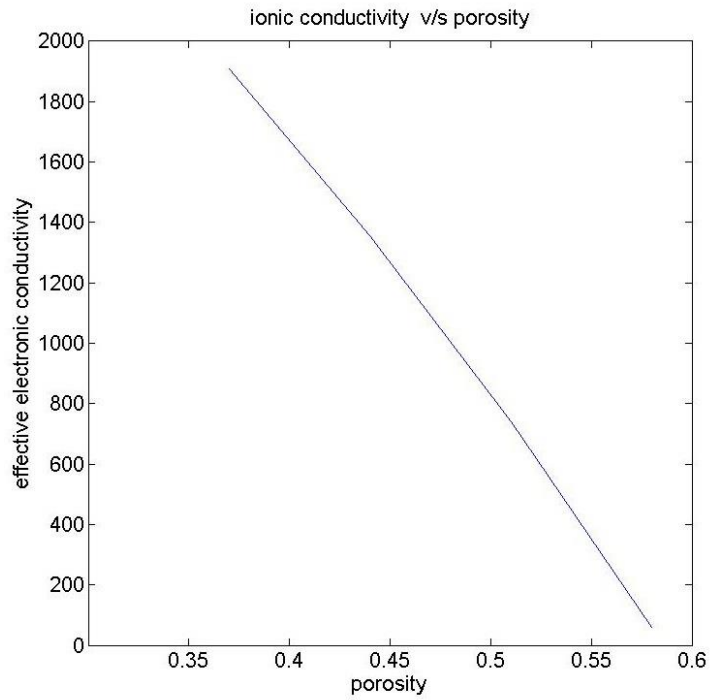
Fig. 13 Electrical conductivity v/s calculated porosity with constant ratio of the ionic and electronic conductor
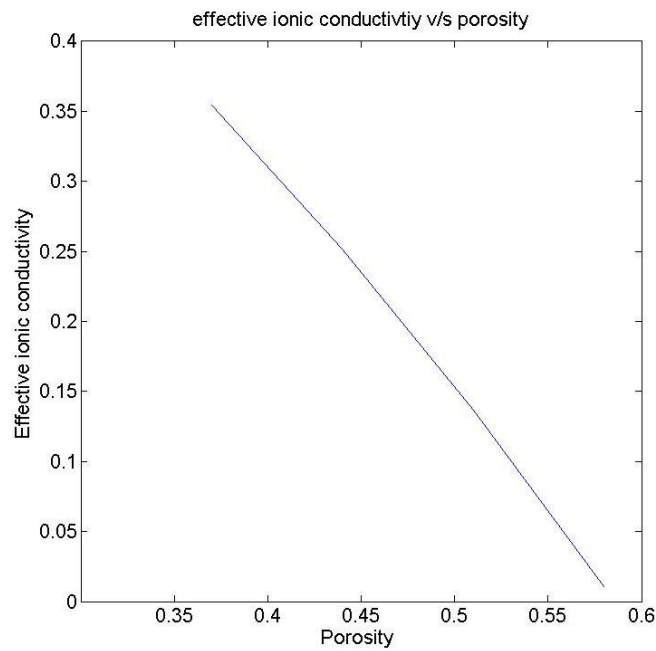


Fig. 14 Ionic conductivity v/s calculated porosity with constant ratio of the ionic and electronic conductor

Figures 13,14 show that with the increment in the porosity and tortuosity we have less electronic and ionic conductivity

And the reason behind going down of these properties is by mixing more and more pore former material we are minimizing the ionic and electronic conductor. And after sintering there we have less contact between the both conductors. Decreasing amount of ionic and electronic conductor makes difficult to be contact of homogenous and heterogeneous conductors. Effect on the properties which shows the contact of both conductors are as figure 15.
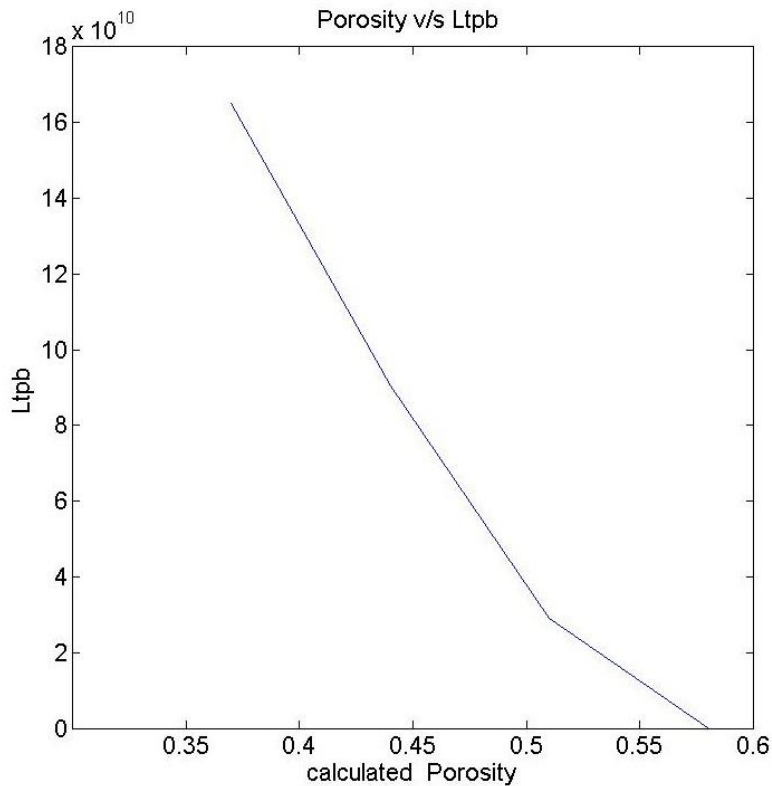


Fig. 15 Length of TPB v/s calculated porosity with constant ratio of the ionic and electronic conductor

The decreasing trend of contact of both conductors and minimizing the possibility of the reaction and decreasing the conductivity of the composite material. With this one more average particle diameter also varies which effects the calculation of permeability of gases through the pores.

Performance of cell after all modelling and simulation can be measure by the performance curve. Basic results we can obtain from the simulation is performance curve which is a plot between the output voltages with current.
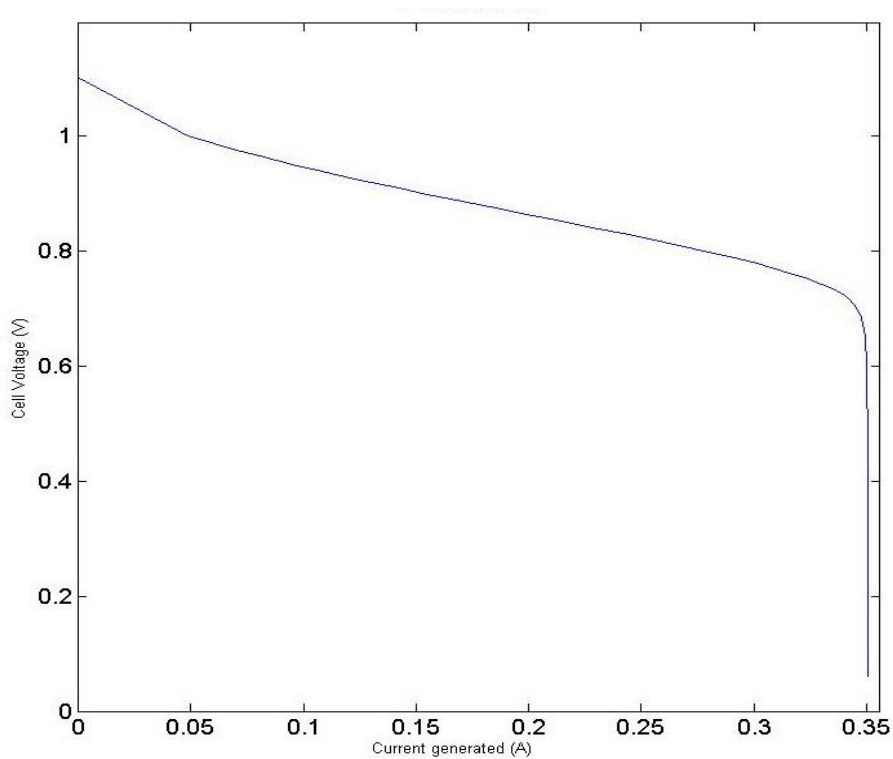


Fig.16   Voltage and current (performance curve) at 800 C and 80 % fuel utilization at 0.8 volt

Figure 16 shows that as we go for higher current our voltage comes down because of losses in the cells. This plot on 800 °C and 80% fuel utilization, operating condition was 97% $H_2$ and 3% $H_2O$ in the fuel and air at atmospheric pressure. The curve is behaving as expected and described in the literatures so we can say that model is behaving fine and we did mass balance also for the model which is also indicates model is behaving correctly.

Fuel cell anode having the electronic and ionic conductor. Compositions of the both particle also effect the cell performance we simulated for the three different composition and generated cell performance
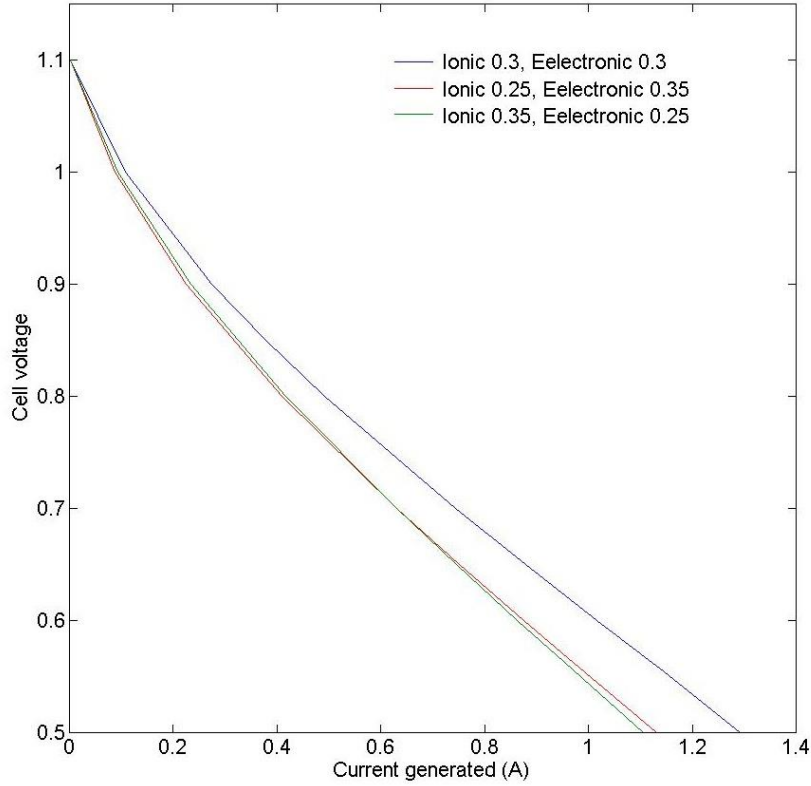
Fig. 17 Performance curve at various composition of the electronic and ionic conductor at constant porosity

Above figure shows that performance of the cell depends on the TPB available. By reducing the one component from the compositions make impact on the contact of ionic and electronic conductor which reduces the TPB and cell performance goes down.

Difference in parameter of cell and performance with different composition of fabrication of anode functional layer can be listed as

| Parameter | $\psi_{io}^{bs} = \psi_{el}^{bs} = 0.30$ | $\psi_{io}^{bs} = 0.25, \psi_{el}^{bs} = 0.35$ | $\psi_{io}^{bs} = 0.35, \psi_{el}^{bs} = 0.25$ |
|---|---|---|---|
| I at 0.8 V , 80 % Uf | 0.49 A | 0.40 A | 0.41 A |
| $\Lambda_{TPB}$ | $1.41 \times 10^{11}$ m$^{-1}$ | $1.38 \times 10^{11}$ m$^{-1}$ | $7.05 \times 10^{10}$ m$^{-1}$ |
| $\sigma_{io}^{eff}$ at anode | 0.36 s/m | 0.18 s/m | 0.51 s/m |
| $\sigma_{el}^{eff}$ at anode | 1961.3 s/m | 2748.4 s/m | 977.57 s/m |
| $\sigma_{io}^{eff}$ at cathode | 0.36 s/m | 0.18 s/m | 0.51 s/m |
| $\sigma_{el}^{eff}$ at cathode | 27.75 s/m | 38.88 s/m | 13.85 s/m |

Table 3 Comparison of cell performance and parameter at different material compositions

In this thesis  parametric study done for the thickness of the functional layers (Anode and Cathode) to see the effect of thickness on the performance curve so we varied the thickness of both in the range of 50-550 micron and obtain the performance curves.
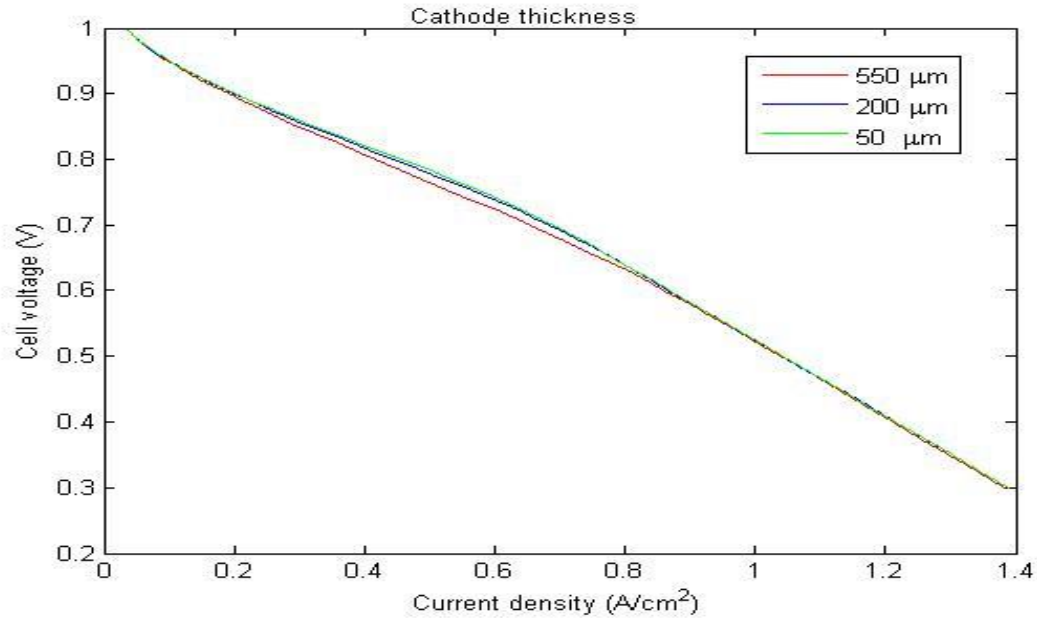


Fig. 18   Performance curve at different cathode thickness at 800 C and 80 % fuel utilization at 0.8 V
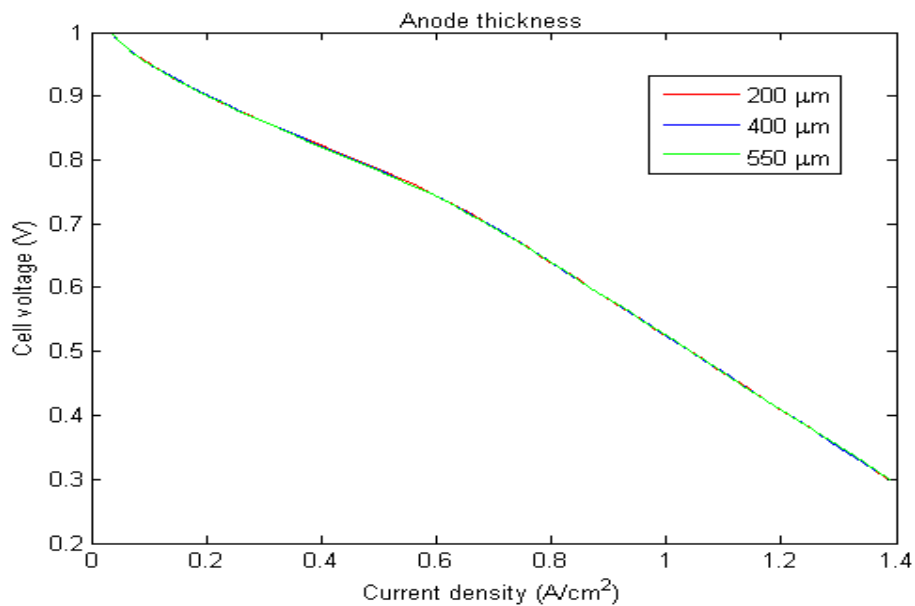
Fig.19 Performance curve at different anode thickness at 800 C and 80 % fuel utilization at 0.8 V

As we can see that the performance curve is not much affected by varying the thickness of both electrodes. The lines of performance are overlapping each other. Reason of this kind of behaviour is near to the electrolyte are more active than which is far from the interface. As we go far from the interface we do not have much reaction in that area and do not contributes much in current generation. Resistance to the ions are much higher in the electrode with respect to the electrolyte. So the ions do not travel much in the electrodes and triple phase boundary formation is also easier to near the electrode electrolyte interface. So the maximum current generation is near to the electrode electrolyte interface. Our next plot explain it better we draw a cut line across the cell and draw the current generation on the different voltages.
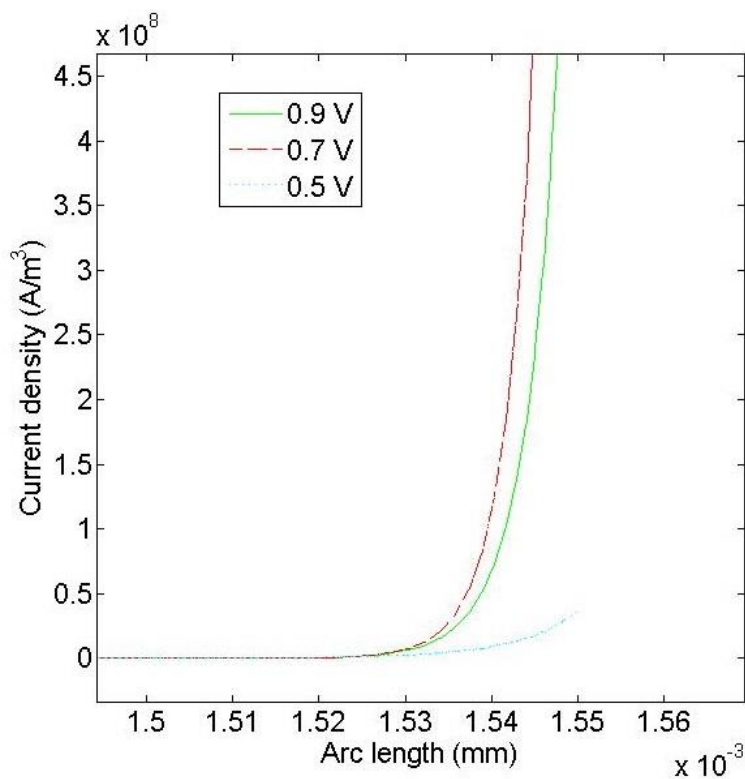


Fig.20 Current generation at different voltage across the cell

Figure 20 is showing that the current generation is only near to the electrode- electrolyte interface. So we can make our electrolytes as much thin as can to reduce the Ohmic losses but we need to make one layer thicker than other to give mechanical strength to the cell in our case we made our anode is thicker.

42

After looking into the cell performance without support layer we introduces the support layer to the cell and it affect the performance of cell.
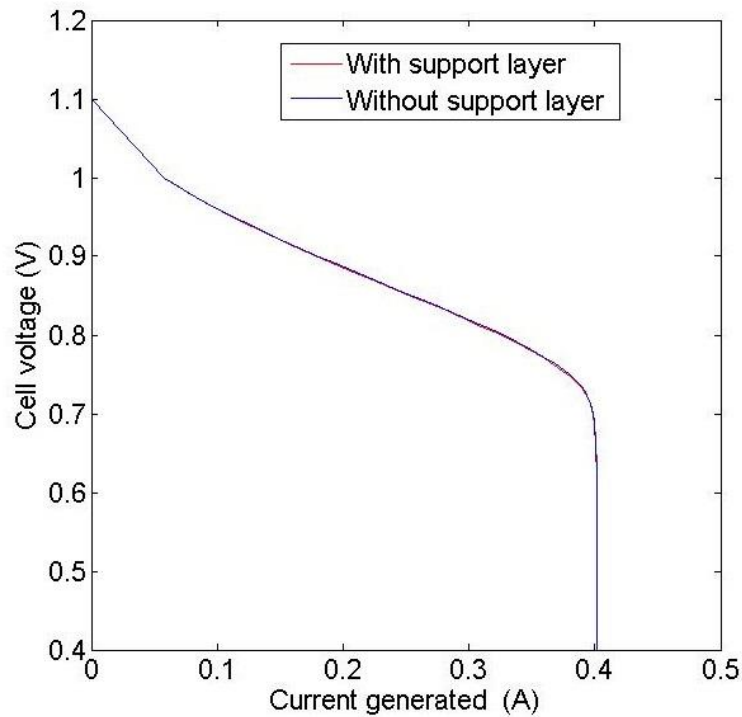


FIG. 21   Comparative performance curve with introduction of anode support layer

This figure shows that the performance of cell with anode support layer and without support layer overlap to each other and son not affect the performance much. So we can fabricate the support layer material with more durable, less resistance offering. From above figure we can conclude that the current generation and performance of cell are not affected by the support layer and its material.

 Effect of temperature on the cell performance so we varied the temperature in the range of (650-800°C).
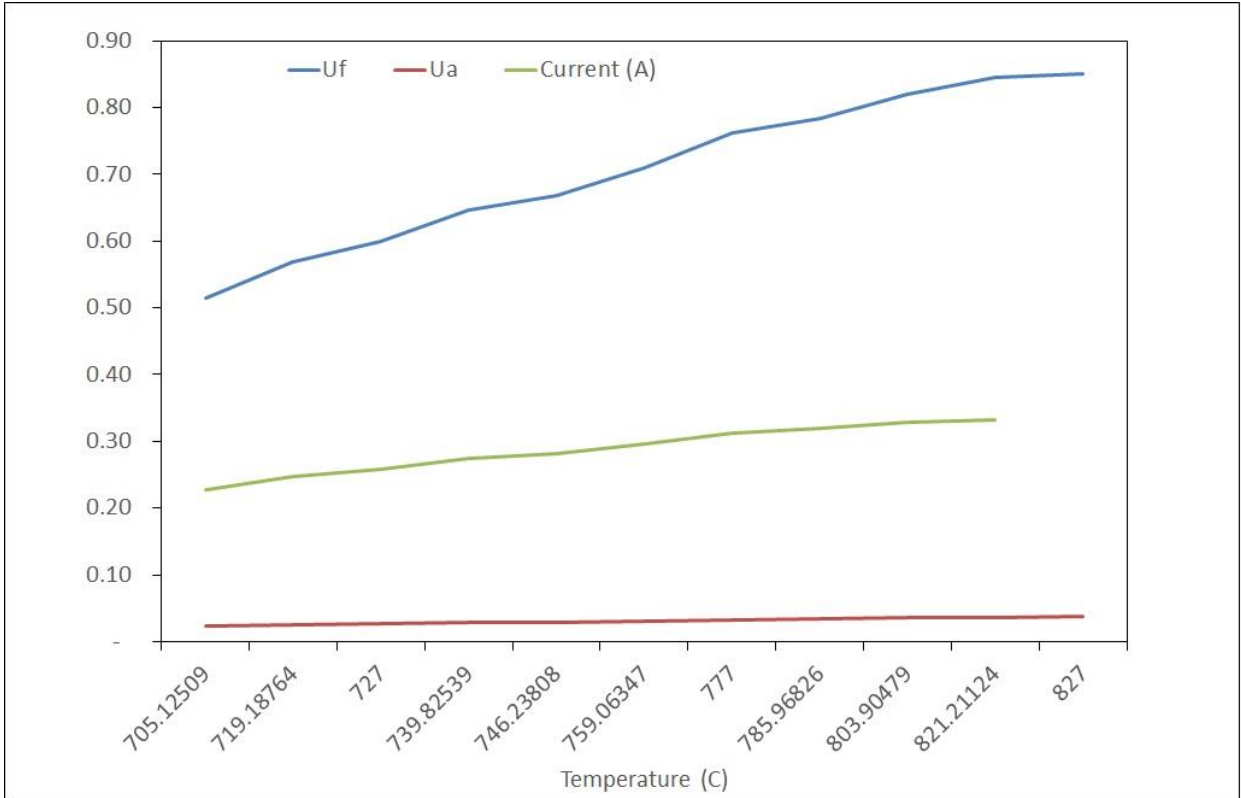
Fig.22 Fuel and air utilization at various temperature with fixed fuel flow rate

Fig 22 shows that with increment in temperature we can see for the same flow rate we have the higher utilization of fuel as well as air. This occurs in cell because of less losses. For getting the higher utilization we need to use the cell at high temperature. Above figure shows the overall performance. To review the more detailed view of effect of temperature we have another plot given below.
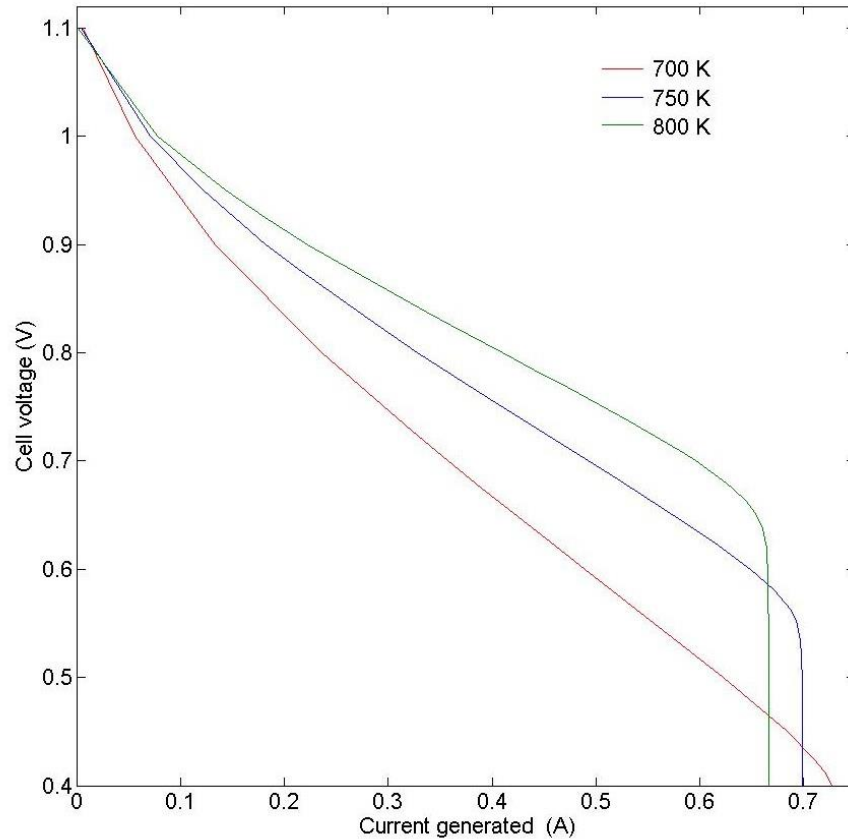
Fig. 23 Performance curve with different temperature at fixed fuel flow rate

Figure 23 shows that with increment in the operating temperature we have better performance and less losses we can get at 650 °C we got less current on the same voltage.

But by increment of 50 °C we are getting more current. SOFC can perform better on the higher temperature but we cannot increase the operating temperature more high thermal stability may be the issue of breakdown of the cell. Reason behind the better performance is at higher temperature we have less activation and Ohmic losses.

Another plot we can look at for the performance of the cell along the cell length we can see the performance of the cell at different temperature
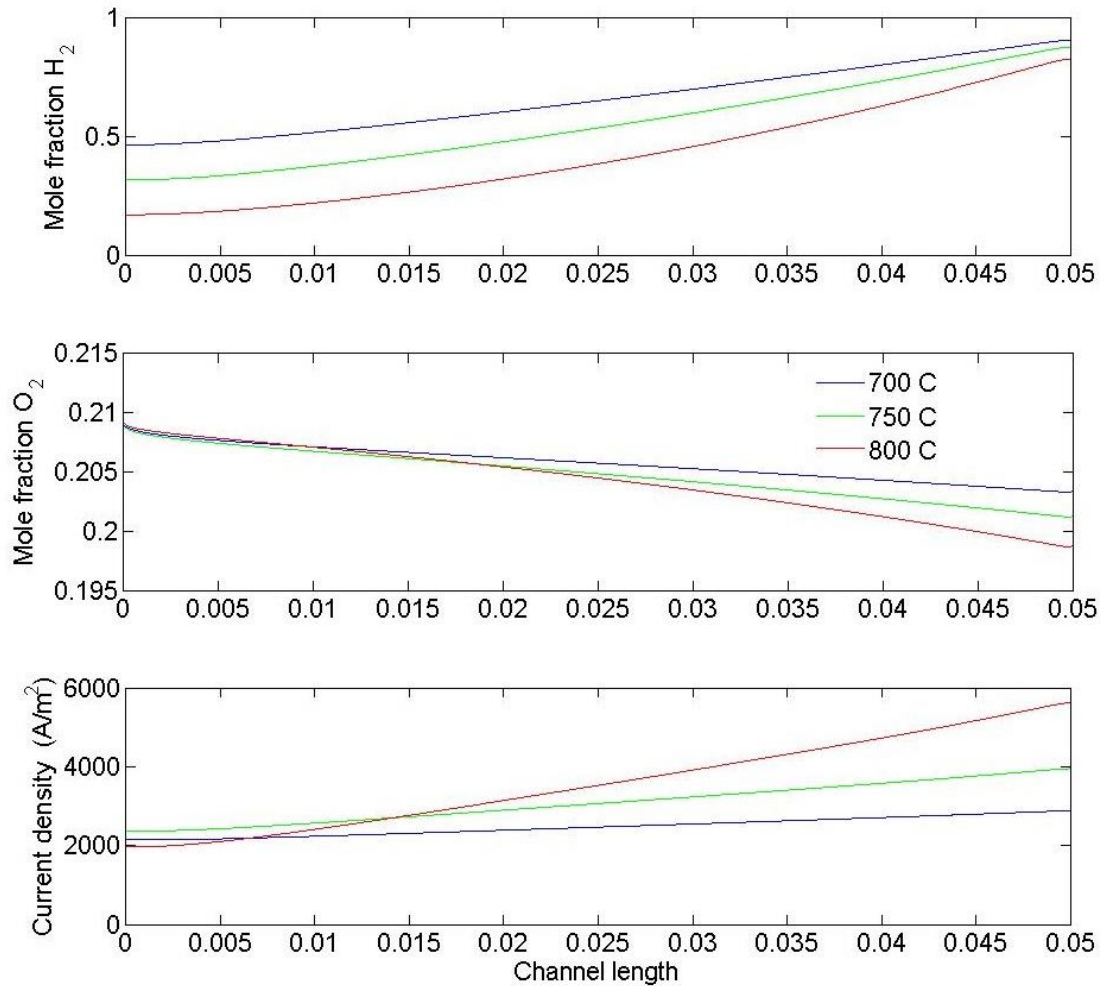
Fig. 24 Current and mole fraction of species at different temperature along the channel at fixed flow rate and inlet concentration of the chemical species.

Figure 24 shows that the performance of cell much better on higher temperature and higher utilization of fuel can achieved and current generation is also better on high temperature

Another parameter velocity of fuel also affect the performance of cell and utilization of fuel and air for getting the effect of fuel velocity we varied the fuel velocity and kept the air velocity constant , got the effect on the fuel utilization , air utilization and the current generation

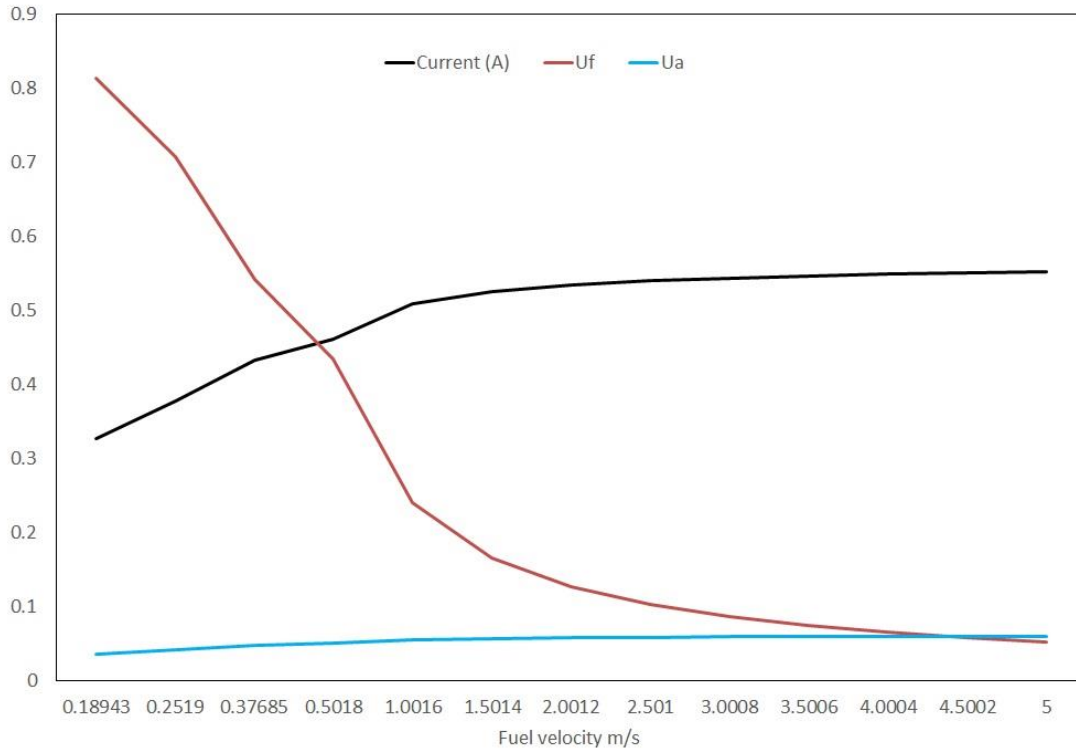Fig. 25 Effect of fuel velocity on the current, fuel utilization and air utilization at constant temperature and inlet concentration

It show that by increasing the fuel velocity we are reducing fuel utilization so for keeping utilization high we need to operate cell at low fuel velocity but with low fuel velocity we need to compromise with current generation.

For looking into the effect of the fuel velocity to the utilization and performance of the cell current generation and behaviour along the cell length we can look into the figure which is plotted by keeping different fuel velocity and utilization parameter and see the current generation and the mole fraction of the fuel and air near to the electrode electrolyte interface.
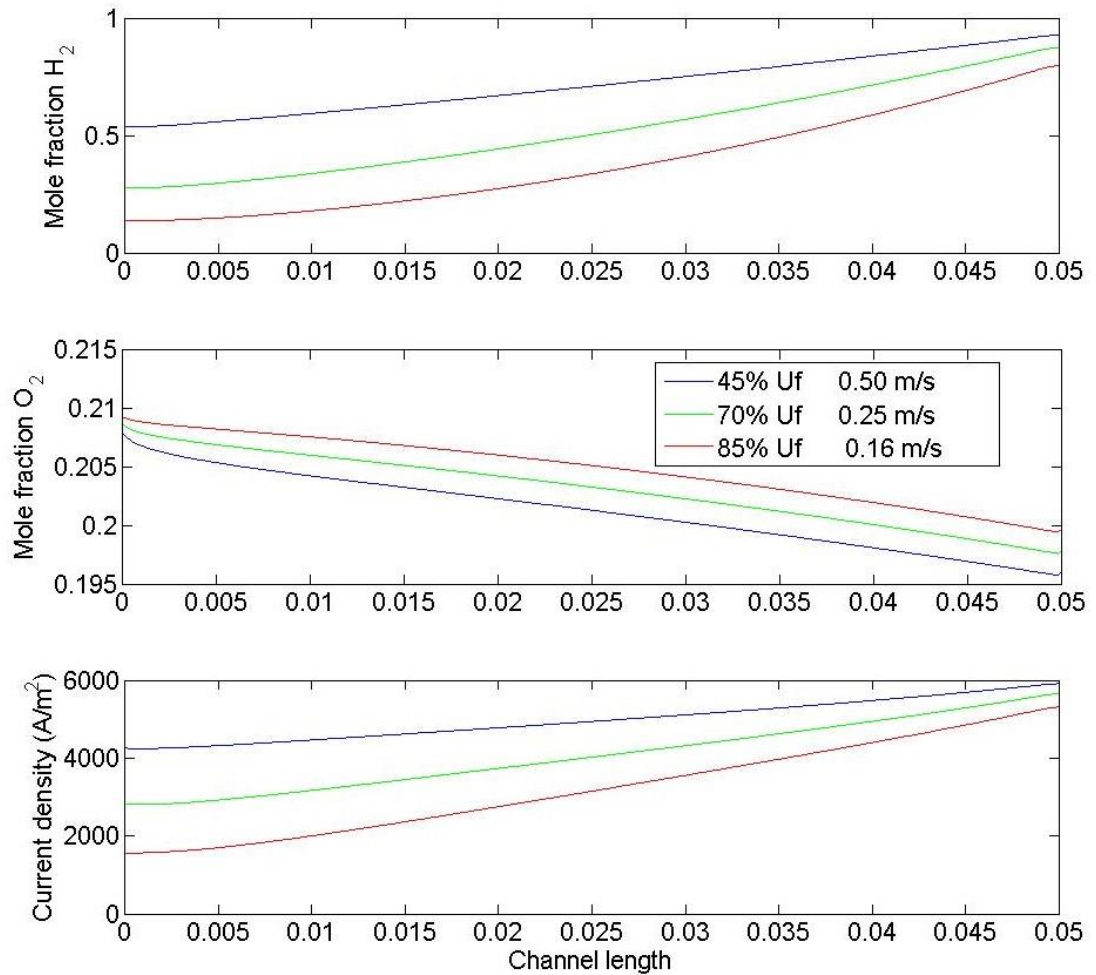
Fig. 26 Effect of utilization on the current and mole fraction of species along length at constant temperature and fixed fuel flow rate

Figure 26 is showing that the lowering the fuel velocity we can achieve the higher utilization but at higher utilization air does not deplete much because we sending the air in execs.at higher utilization fuel is depleting very rapidly but because of fuel depletion half-length of cell is inactive and it not using and current generation is not also uniform throughout the cell length so there may be thermal unevenness also may be there.

In the process of maximizing the utilization there we have main problem arises in the structure of properties is the redox reaction of the nickel metal. In the fuel channel we have the production of the water vapour throughout the channel and it creates the favourable condition for the oxidation of nickel with the reaction of the water vapours. So we examine

the ratio of the partial pressure of hydrogen and water vapours in various conditions. First we can look ratio of water vapour to the hydrogen along the channel length. We observed at the high current and high utilization and the limit of the 0.7 V, if we decrease the voltage we can see at 0.69 V reached to the limit where nickel oxidation started. And we can see the near to fuel outlet 0.4 cm length of the cell offer the favourable condition to the nickel oxidation.
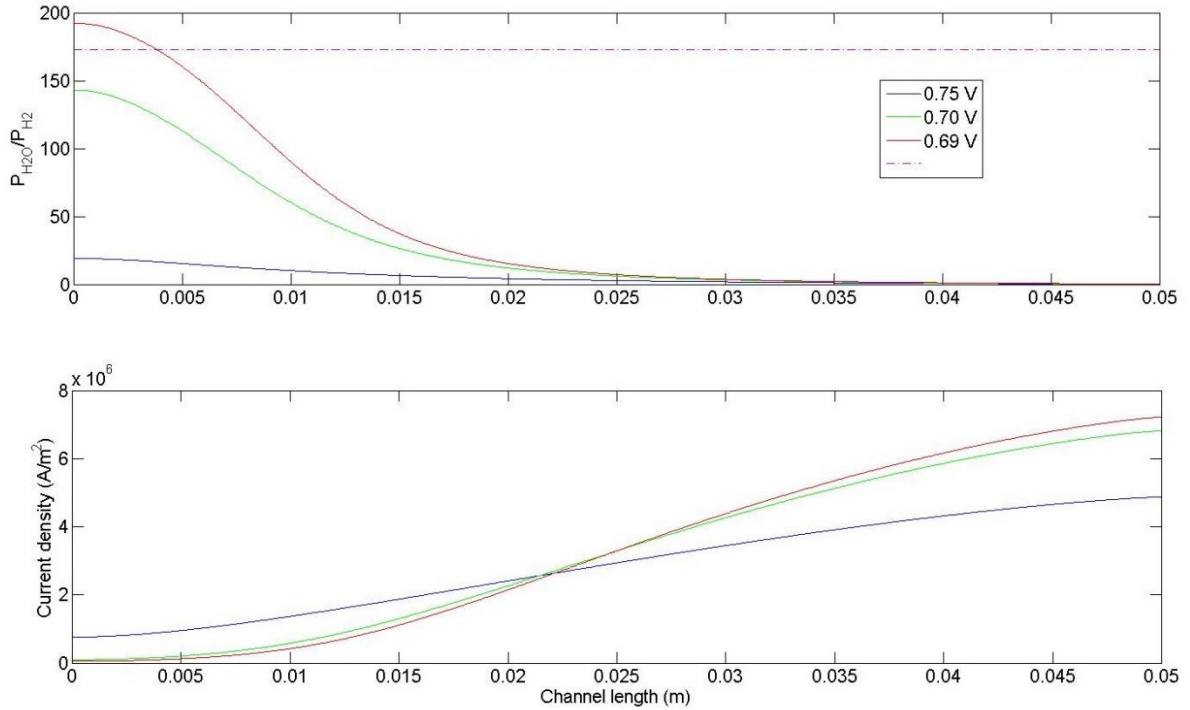


Fig. 27 ratio of partial pressure along the cell length with fixed fuel flow rate and operating temperature

The ratio along the channel length with different fuel utilization
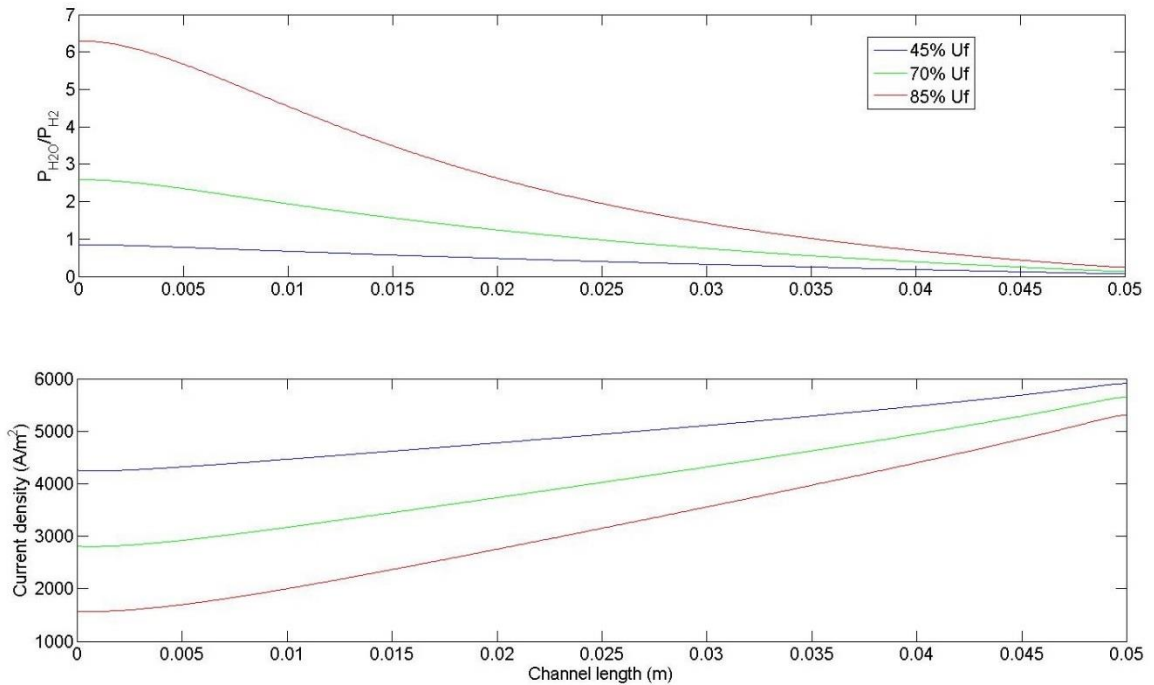


Fig .27 Ratio of partial pressure of hydrogen to water vapour along the cell length with
varying fuel utilization at constant temperature and fuel inlet composition, fuel inlet is on the
right side

Figure 27 shows that with the increment of fuel utilization we will have lower ratio of
hydrogen to the water vapours and gives the favourable condition to the nickel oxidation. So
we can operates the cell at very high utilization with nickel catalyst. So we can use the
recycling of the fuel to increase the utilization of the cell.

With temperature variation also we can see the variation in the Prat. As we discussed before
increase the temperature we will have higher utilization and with the higher utilization we
will have the nickel oxidation at the end of the cell.
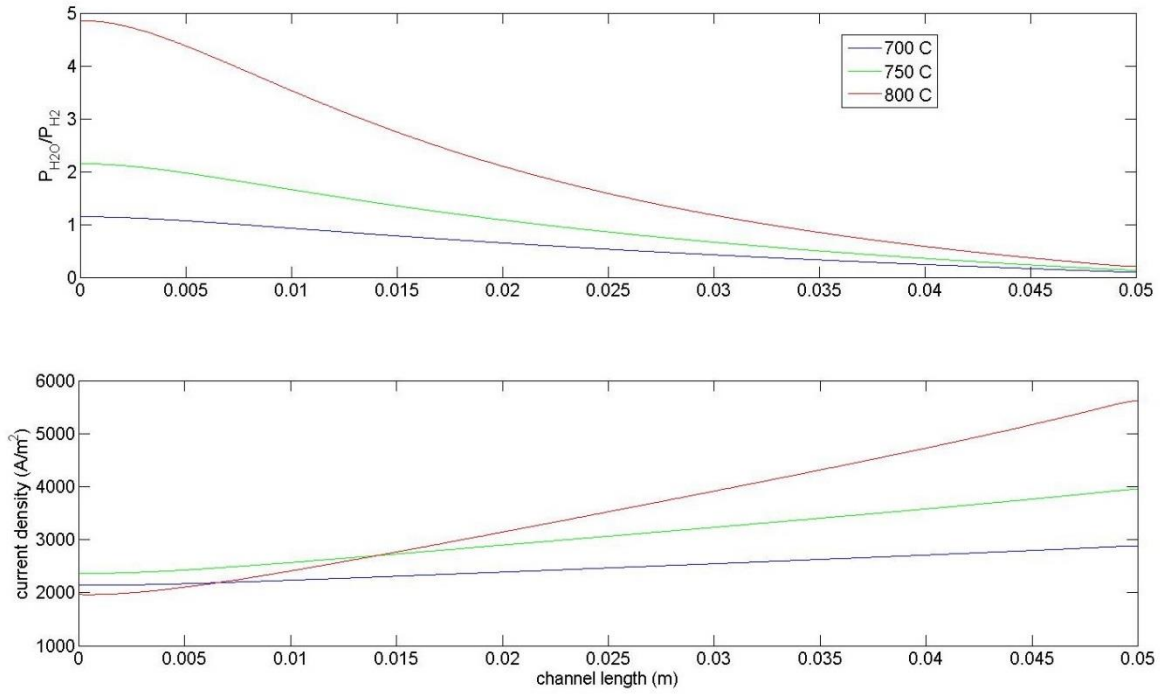
Fig. 28   Ratio of partial pressure of hydrogen and water vapour along channel length with varying temperature at fixed fuel flow rate and fuel inlet concentration, fuel inlet is right side.

# Conclusions

This thesis presented the 2-D model of anode supported solid oxide fuel cell. The effective properties of the various layers are functions of composition, and the model included all important physics except for heat transfer. This model is a fully coupled detailed reaction-transport model of solid oxide fuel cell operation.

To ensure the cell behaviour is modelled adequately, the cell has been simulated for various ranges of design and operating parameters and the mass balance for both the air and fuel sides was verified. The expected effect of physical properties on cell performance was also verified.

After modelling the cell and simulating for the various parameters, we can conclude some points from the results:-

1. Variation of thicknesses of the anode and cathode (50μm to 500μm) do not affect the performance of the cell. This happens because the higher density of active sites (TPB) will only help in performance near the electrode-electrolyte interface only. In the results we observe ~20μm thickness is responsible for the current generation because of high ionic conductive resistance in both electrodes. Thus the electrodes need not be thicker than this value. Of course mechanical constraints dictate that at least one layer be thick enough to ensure mechanical stability and thus the anode includes a 0.5 mm thick support layer which is shown not to adversely afect the cell performance.

2. Fuel inlet velocity has a significant effect on the fuel utilization. By decreasing the fuel velocity we can see that the utilization increases. For higher fuel inlet velocity there we do not have significant concentration gradient along the channel length but for lower fuel velocity we can see the development of a considerable concentration gradient along the channel length. This means that the average fuel concentration at the reactive sites in the anode is lower at a lower fuel inlet velocity. Thus, the operation of the cell at low fuel inlet velocities causes a decrease in  total current generation due to the above effect.

3. Operating temperature is the parameter which effect the cell performance significantly. At higher temperature we can see better performance of the cell. Parameters such as ionic conductivity, exchange current density and diffusivity of the chemical species increase with increasing temperature which enhances cell performance. Fuel utilization and

current generation both increase simultaneously with temperature if the fuel inlet velocity is kept constant.

4. Fabrication of electrode with various volume fraction of the pore former, electronic conductor and ionic conductor give the different value for the microstructural properties. An equal volume fraction of the electronic and ionic conductor gives the best performance for the cell because equal amounts of the both conductors give the highest reaction site density (TPB). Higher reaction site help to increase the exchange current density. The effect of changing the composition on the $\sigma_{el}^{eff}$ , $\sigma_{io}^{eff}$ is not significant enough to counter the above effect on exchange current density.

5. With parametric study for the fuel utilization we can observe that the ratio in the partial pressure of hydrogen and water vapour decrease along the cell length at very high fuel utilization. High ratio of the $P_{H2O}/P_{H2}$ promotes the oxidation of the nickel. To prevent the oxidation of nickel we should keep the ratio below the threshold dictated by the thermodynamics of Ni oxidation. From this work we can say that Ni oxidation seems to become favourable only at very severe conditions. For example, at 800ºC, for a fuel velocity that gives $U_f$ =80% at 0.8 V, lowering the cell voltage below 0.7 V drives $U_f$ above 99%. It is only at these very severe conditions that Ni oxidation becomes favourable in the last 4 mm of the fuel channel.

Future work will focus on a closer investigation of the high fuel utilization regimes in SOFCs with an aim to describe a safe envelope of operating conditions that maximize fuel utilization while ensuring that the Ni in the anode is protected from oxidation.

# References

1. Zhu, H., & Kee, R. J. (2008). Modeling Distributed Charge-Transfer Processes in SOFC Membrane Electrode Assemblies. *Journal of The Electrochemical Society*, *155*(7), B715. doi:10.1149/1.2913152

2. Vogler, M., Bieberle-Hütter, A., Gauckler, L., Warnatz, J., & Bessler, W. G. (2009). Modelling Study of Surface Reactions, Diffusion, and Spillover at a Ni/YSZ Patterned Anode. *Journal of The Electrochemical Society*, *156*(5), B663. doi:10.1149/1.3095477

3. Kumar, S. (2013). A fully coupled transport-reaction model for a solid oxide fuel cell, M.Tech. thesis, I.I.T. Hyderabad, India.

4. Polisetty, V. G. (2013). State Estimation in Solid Oxide Fuel Cell (SOFC) system,

5. M.Tech. thesis, I.I.T. Hyderabad, India.

6. Faes, A., Hessler-Wyser, A., Zryd, A., & Van herle, J. (2012). A Review of RedOx Cycling of Solid Oxide Fuel Cells Anode. *Membranes*, *2*(4), 585–664. doi:10.3390/membranes2030585

7. Hardjo, E. F. (2012). Numerical model of Ni-infiltrated porous anode solid oxide fuel cells. M.Sc. Thesis, Queens University, Canada.

8. Charette, G. G., & Flengas, S. N. (1968). Thermodynamic Properties of the Oxides of Fe, Ni, Pb, Cu, and Mn, by EMF Measurements. *Journal of The Electrochemical Society*, *115*(8), 796. doi:10.1149/1.2411434

9. Lim, H.-T., Cheol Hwang, S., & Ahn, J. S. (2013). Performance of anode-supported solid oxide fuel cell in planar-cell channel-type setup. *Ceramics International*, *39*, S659–S662. doi:10.1016/j.ceramint.2012.10.156

10. Bertei, A., Barbucci, A., Carpanese, M. P., Viviani, M., & Nicolella, C. (2012). Morphological and electrochemical modeling of SOFC composite cathodes with distributed porosity. *Chemical Engineering Journal*, *207-208*, 167–174. doi:10.1016/j.cej.2012.06.034

11. COMSOL. COMSOL Multiphysics help documentation, COMSOL 4.3b, 2013.